

A Minimax Framework for Two-Agent Scheduling with Inertial Constraints

Feihong Yang, *Graduate Student Member, IEEE*, and Yuan Shen, *Senior Member, IEEE*

Abstract—Autonomous agents are promising in applications such as intelligent transportation and smart manufacturing, and scheduling of agents has to take their inertial constraints into consideration. Most current researches require the obedience of all agents, which is hard to achieve in non-dedicated systems such as traffic intersections. In this article, we establish a minimax framework for the scheduling of two inertially constrained agents with no cooperation assumptions. Specifically, we first provide a unified and sufficient representation for various types of situation information, and define a state value function characterizing the agent's preference of states under a given situation. Then, the minimax control policy along with the calculation methods is proposed which optimizes the worst-case state value function at each step, and the safety guarantee of the policy is also presented. Furthermore, several generalizations are introduced on the applicable scenarios of the proposed framework. Numerical simulations show that the minimax control policy can reduce the largest scheduling cost by 13.4% compared with queuing and following policies. Finally, the effects of decision period, observation period and inertial constraints are also numerically discussed.

Index Terms—Minimax scheduling, inertial constraints, distributed control.

I. INTRODUCTION

Advancing communication and control technologies enable the proliferation of autonomous agents such as robots, intelligent vehicles and unmanned aerial vehicles (UAVs). Compared with static devices, their dynamics greatly extend the scope of industrial and civil applications to scenarios including environment sensing, intelligent transportation and smart manufacturing [1]–[6]. In multi-agent systems, abundant coordination and competition schemes can be developed for different tasks, which attract massive attention in various researches [7]–[10].

When multiple agents in a system require a limited resource, scheduling schemes are necessary to avoid conflicts, as shown in Fig. 1(a). The research of scheduling problems has a long history [11]–[14], where the scheduling is traditionally modelled as optimization problems over the occupation time periods of the agents, and commonly-used metrics include (maximum or average) completion time and lateness. In recent studies of wireless communications, scheduling problems are also widely considered over data packets [15]–[18], and some new metrics such as age of information, system capacity and energy consumption are proposed.

The authors are with the Department of Electronic Engineering, Tsinghua University, and Beijing National Research Center for Information Science and Technology, Beijing 100084, China (e-mail: yfh17@mails.tsinghua.edu.cn, shenyuan_ee@tsinghua.edu.cn).

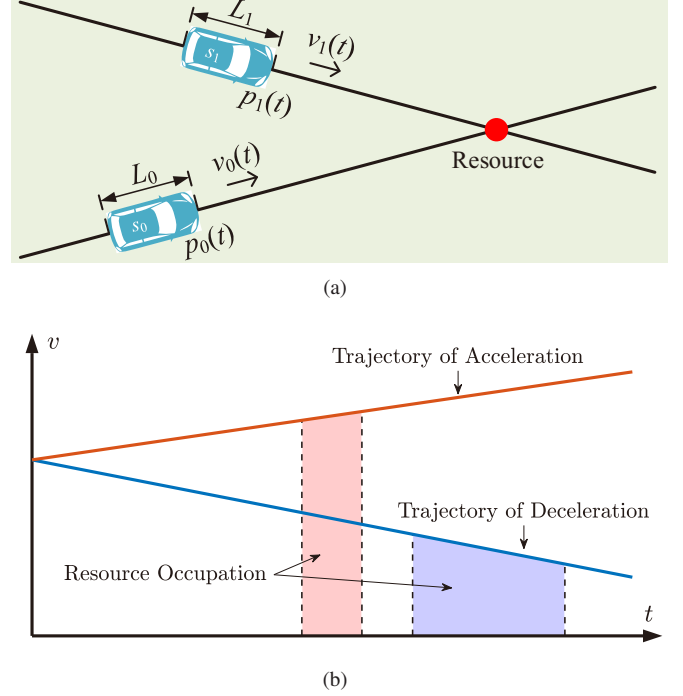


Fig. 1: (a) Two agents requiring a unique resource. (b) For an agent with inertial constraints, choosing different trajectories can result in different durations of the resource occupation. As a comparison, agents without inertial constraints can always reach the highest velocity in an instant, and the resource occupation durations can be regarded as a constant.

However, it is a different issue when the resource is space-related and the autonomous agents are constrained by inertia when approaching the resource, and one typical scenario is a traffic intersection in an intelligent transportation system (ITS). In this case, we cannot model agents by a set of time parameters such as the arrival time and the resource occupation duration as traditional scheduling problems, since these parameters are no longer predetermined and rely on the trajectories of agents, as shown in Fig. 1(b). Instead, the spatial states of the agents need to be characterized in the modelling including their positions and velocities, and detailed agent trajectories need to be generated in a scheduling policy besides the time slot assignments of the resource. Furthermore, since the velocities of agents during the occupation is not constant, they should also be considered when evaluating the scheduling performance.

There are some works taking the inertial constraints into consideration, a large portion of which lie under the scenario

of scheduling intelligent vehicles near traffic intersections [19], [20]. Generally, these researches can be divided into two main categories. The first category applies a hybrid framework, where the occupation time periods (possibly with redundancy) or an occupation order is firstly assigned to the agents by a central device, and then the control policies are designed for single agents to meet the requirements. Specifically, protocols such as adaptive traffic lights [21]–[25], time slot reservation [26]–[29] and central optimization [30]–[34] are analyzed to complete the first step of scheduling. Furthermore, there are also some researches focusing on the distributed implementations of these protocols [35]–[37], in which the central device can be removed. Another category contains the trajectory planning frameworks, which directly return the non-conflicting trajectories of all agents without intermediate steps using methods including characterizing the maximal controlled invariant set [38], [39] and performing optimization over the control inputs [40]–[44].

However, most of current researches are based on the assumption that all agents in the system follow the proposed protocol, while loading the protocol to all agents often costs much in a complex system, and is sometimes impossible in non-dedicated systems such as traffic intersections containing human-driven vehicles. As long as a disobedient agent exists, the safety of the system cannot be guaranteed. Exceptions such as [31], [35], [38] allow the existence of non-autonomous agents, while they only focus on finding a collision avoiding solution without considering the scheduling performance.

In this article, we consider the scheduling problem of inertially constrained agents from the one-agent perspective, to which the other agents are not necessarily cooperative. Specifically, we adopt the two-agent model for simplicity, which is sufficient to illustrate the main idea and obtain non-trivial insights. The contributions of this article are as follows.

- We propose a scheduling framework taking the acceleration limits of agents into account and develop a unified and sufficient representation of various types of situation information for the scheduling of an agent.
- We establish a state value function for an agent based on its obtained situation information by minimizing the manageable component of the accessible cost, which characterizes its preference of different states for the scheduling.
- We develop a minimax control policy for the scheduling problem which accords with the intuition of moving toward the state with the best worst-case preference, and further prove the safety guarantee of the policy and verify its robust performance by comparing with other typical policies through numerical simulations.

The rest of the article is organized as follows. Section II formulates the two-agent scheduling problem by introducing the scheduling cost. Then in Section III, we characterize the unified representation of situation information and propose the state value function under a fixed situation. The minimax control policy is established in Section IV along with the safety guarantee and the calculation methods. Section V provides intuitions and several generalizations of the framework, and

Section VI presents numerical results on the state value function and the scheduling performance of the proposed policy. Finally, the article is concluded in Section VII.

Notations: Throughout the article, when we want to refer to a variable, such as $p_i(t)$ (the position of agent i at time t), with emphasizing the corresponding trajectory which, for example, is denoted by σ , we use the notations with superscript σ , such as $p_i^\sigma(t)$. We use (a, b) and $[a, b]$ to represent an open interval and a closed interval, respectively, and $\langle a, b \rangle$ is used to represent an ordered pair to avoid ambiguity. For a set \mathcal{A} , $\text{card}(\mathcal{A})$ represents its cardinality and $\mu(\mathcal{A})$ represents its Lebesgue measure. For equations, “ \triangleq ” is used when one side is undefined and it represents the definition of this side.

II. MODELLING AND PROBLEM FORMULATION

In this section, we introduce the system model and formulate the scheduling problem of two inertially constrained agents.

A. System Model

Consider a system with two agents s_0 and s_1 , both of which move along a given track and require a unique resource in some future stages, as illustrated in Fig. 1(a).¹ For each agent s_i ($i \in \{0, 1\}$), an axis is attached to characterize its movement, where the origin is always set to be the position of the resource. Let L_i be the resource demand of the agent s_i under its own axis, and let $p_i(t)$, $v_i(t)$ and $a_i(t)$ be the position, velocity and acceleration of s_i at time t , respectively. Therefore, the resource is occupied by s_i at time t if and only if $p_i(t) \in (0, L_i)$.

Furthermore, we impose the following two kinematic constraints on the two agents that for $i \in \{0, 1\}$ and $t \in \mathbb{R}_+$,

$$0 \leq v_i(t) \leq v_M \quad (1)$$

$$-a_{i,m} \leq a_i(t) \leq a_{i,M} \quad (2)$$

where v_M , $a_{i,m}$, $a_{i,M}$ are positive numbers.² Specifically, note that (2) is the *inertial constraint* which is common among physical agents. Under the two constraints (1) and (2), we can regard the pair

$$\mathbf{x}_i(t) \triangleq \langle p_i(t), v_i(t) \rangle \quad (3)$$

as the *state* and regard $a_i(t)$ as the *control* of s_i at time t .

To ensure the safety of the system, we do not allow the two agents to simultaneously occupy the resource, i.e.,

$$\text{card}\{i \mid p_i(t) \in (0, L_i)\} \leq 1, \quad \forall t \geq 0. \quad (4)$$

Furthermore, by defining

$$t_{i,\text{in}} \triangleq \inf\{t \mid p_i(t) > 0\} \quad (5)$$

$$t_{i,\text{out}} \triangleq \sup\{t \mid p_i(t) < L_i\} \quad (6)$$

¹The intersection shown in Fig. 1(a) is a topological intersection instead of a geometric one. In other words, issues such as the intersection angle of the tracks or the widths of the agents are beyond the scope of the article.

²Without loss of generality, the maximum velocity constraint v_M is set to be equal for the two agents, which can be achieved by rescaling the axis of either agent.

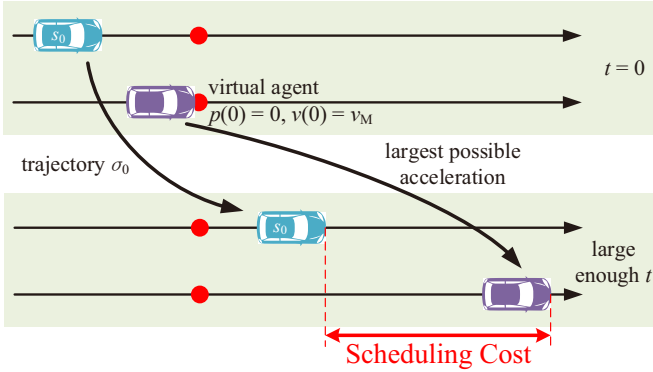


Fig. 2: Intuition of the scheduling cost $C(\sigma_0; t_{1,\text{in}}, t_{1,\text{out}})$.

for $i \in \{0, 1\}$, the safety condition is equivalent to

$$(t_{0,\text{in}}, t_{0,\text{out}}) \cap (t_{1,\text{in}}, t_{1,\text{out}}) = \emptyset. \quad (7)$$

Therefore, scheduling is required in order to meet the safety condition.

B. Formulation of the Scheduling Problem

In this article, we consider the scheduling problem from the perspective of the agent s_0 . In other words, we can only control s_0 and know nothing about the future control of s_1 . Nevertheless, we assume that the constraints (1) and (2) are known by s_0 . Furthermore, s_0 is allowed to obtain information on history or current states of s_1 by observation or by communication with other possible cooperative devices. However, due to the non-ideal environment, observation or communication may suffer from failure and delay, and thus s_0 cannot predict when and which information can be successfully obtained in the future.

To ensure the existence of a safe scheduling, we assume that s_0 is able to stop before the resource. In other words, the initial state of s_0 satisfies

$$p_0(0) + \frac{v_0(0)^2}{2a_{0,m}} \leq 0. \quad (8)$$

We aim at developing a causal control policy for s_0 which generates a trajectory with a low scheduling cost. Specifically, we consider a discrete set of decision times $\{t_k | k \geq 0\}$ with $t_0 = 0$ and $t_k < t_{k+1}$ for any $k \geq 0$. Then at each decision time t_k , the policy can make use of all collected causal information and return the trajectory of s_0 on the next time period $[t_k, t_{k+1}]$. Now we define the scheduling cost of s_0 under a fixed trajectory of s_1 .

Definition 1 (Scheduling Cost): Fix the trajectory of s_1 . Then for a given trajectory σ_0 of s_0 , the scheduling cost is defined by

$$C(\sigma_0; t_{1,\text{in}}, t_{1,\text{out}}) \triangleq \begin{cases} v_M t_{0,\text{in}}^{\sigma_0} + \frac{1}{2a_{0,m}} (v_M - v_0^{\sigma_0}(t_{0,\text{in}}^{\sigma_0}))^2, & \text{if } (t_{0,\text{in}}^{\sigma_0}, t_{0,\text{out}}^{\sigma_0}) \cap (t_{1,\text{in}}, t_{1,\text{out}}) = \emptyset; \\ +\infty, & \text{otherwise.} \end{cases} \quad (9)$$

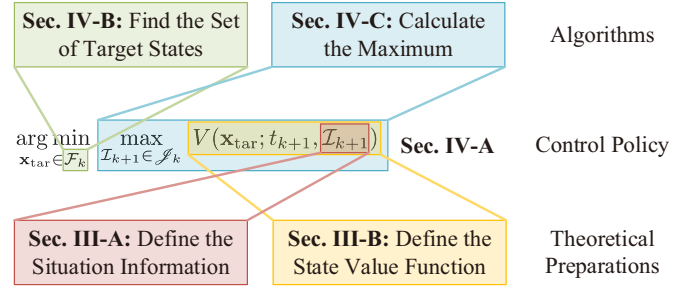


Fig. 3: Sketch of the article.

According to (9), only the control before $t_{0,\text{in}}$ makes a difference to the cost as long as the safety condition is satisfied. For completeness, we always set the control of s_0 to be

$$a_0(t) = a_{0,A}(t) \triangleq \begin{cases} a_{0,M}, & \text{if } v_0(t) < v_M; \\ 0, & \text{if } v_0(t) = v_M \end{cases} \quad (10)$$

for $t \geq t_{0,\text{in}}$, which is always a good choice to reduce $t_{0,\text{out}}$ and decrease the possibility of conflict.³

Furthermore, note that when the safety condition holds, the cost is in unit of distance and can be divided into two parts, which can be regarded as the “time cost” related to $t_{0,\text{in}}$ and the “velocity cost” related to $v_0(t_{0,\text{in}})$, respectively. This definition is intuitive since a earlier occupation time and a quicker occupation velocity implies a higher scheduling efficiency. It can also be interpreted as the final distance between s_0 with a virtual agent which starts from the state $p(0) = 0, v(0) = v_M$ and always follows the largest possible acceleration, as shown in Fig. 2.

In summary, the scheduling problem we consider in this article can be formulated as follows.

Problem: Designing a causal control policy for the agent s_0 to reduce the scheduling cost $C(\sigma_0; t_{1,\text{in}}, t_{1,\text{out}})$, where σ_0 is the output trajectory of the policy.

C. Sketch of the Article

Due to the causality constraint, $t_{1,\text{in}}$ and $t_{1,\text{out}}$ are unknown in advance, and thus the scheduling cost $C(\sigma_0; t_{1,\text{in}}, t_{1,\text{out}})$ cannot be directly accessed by s_0 . To tackle the difficulty, we propose a control policy (Algorithm 1) in Section IV-A, in which the most crucial step is solving a minimax optimization problem (34). Intuitively, under the proposed policy, s_0 always moves toward the state with higher preference based on its currently obtained situation information.

The sketch of the article is shown in Fig. 3. We first formulate and analyze the concepts of “situation information” and “preference of states” in Section III as theoretical preparations. Then we establish the minimax control policy and provide the safety guarantee in Section IV-A. After that, algorithms for the implementation of the policy are developed.

³Note that this is only the restriction of the trajectory of s_0 . We cannot make the similar assumption for s_1 since we have no control of it.

III. THEORETICAL PREPARATIONS

In this section, we characterize the obtained situation information from various sources with a unified form denoted by \mathcal{I} , and then establish the state value function for a given situation.

Recall that all trajectories considered in this article need to satisfy the kinematic constraints (1) and (2). For convenience, we first provide some definitions on the agent trajectories.

Definition 2 (Trajectory Set): Let $t_0 \geq 0$ and $\mathbf{x} = \langle p, v \rangle$ with $0 \leq v \leq v_M$. Then for an agent s_i , define

$$\Sigma_i(\mathbf{x}; t_0) \triangleq \left\{ \sigma \left| \begin{array}{l} \mathbf{x}_i^\sigma(t_0) = \mathbf{x} \\ 0 \leq v_i^\sigma(t) \leq v_M, \forall t \geq 0 \\ -a_{i,m} \leq a_i^\sigma(t) \leq a_{i,M}, \forall t \geq 0 \end{array} \right. \right\} \quad (11)$$

be the set of all trajectories of s_i with the state \mathbf{x} at time t_0 .

Definition 3 (Typical Trajectories): Let $\mathcal{T} \subseteq \mathbb{R}_+$ be an interval and let

$$a_{i,A}(t) \triangleq \begin{cases} a_{i,M}, & \text{if } v_i(t) < v_M; \\ 0, & \text{if } v_i(t) = v_M \end{cases} \quad (12)$$

$$a_{i,D}(t) \triangleq \begin{cases} -a_{i,m}, & \text{if } v_i(t) > 0; \\ 0, & \text{if } v_i(t) = 0. \end{cases} \quad (13)$$

Then a trajectory σ of s_i is called

- a DEC trajectory on \mathcal{T} , if $a_i^\sigma(t) = a_{i,D}(t)$ for all $t \in \mathcal{T}$;
- an ACC trajectory on \mathcal{T} , if $a_i^\sigma(t) = a_{i,A}(t)$ for all $t \in \mathcal{T}$;
- a DEC-ACC trajectory on \mathcal{T} , if there exists $t_D^\sigma \in \mathcal{T}$, such that $a_i^\sigma(t) = a_{i,D}(t)$ for $t \in \mathcal{T} \cap (0, t_D^\sigma)$ and $a_i^\sigma(t) = a_{i,A}(t)$ for $t \in \mathcal{T} \cap (t_D^\sigma, +\infty)$;
- an ACC-DEC trajectory on \mathcal{T} , if there exists $t_A^\sigma \in \mathcal{T}$, such that $a_i^\sigma(t) = a_{i,A}(t)$ for $t \in \mathcal{T} \cap (0, t_A^\sigma)$ and $a_i^\sigma(t) = a_{i,D}(t)$ for $t \in \mathcal{T} \cap (t_A^\sigma, +\infty)$.

A. Information Extraction

In this subsection, we fix the current time t_{cur} and aim at extracting useful information for the scheduling task of s_0 . We assume that $p_0(t_{\text{cur}}) \leq 0$; otherwise, the scheduling is unnecessary. Furthermore, the following technical assumption is made to avoid the infinite occupation time of s_1 .

Assumption 1: $t_{1,\text{out}} \leq B$, where B is a large enough positive number.

Note that $p_0(t_{\text{cur}}) \leq 0$ implies $t_{\text{cur}} \leq t_{0,\text{in}} \leq t_{0,\text{out}}$. According to the scheduling cost defined in (9), it is easy to check that

$$C(\sigma_0; t_{1,\text{in}}, t_{1,\text{out}}) = C(\sigma_0; \hat{t}_{1,\text{in}}, \hat{t}_{1,\text{out}}) \quad (14)$$

where

$$\hat{t}_{1,\text{in}} \triangleq \max\{t_{1,\text{in}}, t_{\text{cur}}\}, \quad \hat{t}_{1,\text{out}} \triangleq \max\{t_{1,\text{out}}, t_{\text{cur}}\}. \quad (15)$$

In other words, all information that s_0 needs for its scheduling at time t_{cur} is contained in the pair $\langle \hat{t}_{1,\text{in}}, \hat{t}_{1,\text{out}} \rangle$.

Although the exact value of $\langle \hat{t}_{1,\text{in}}, \hat{t}_{1,\text{out}} \rangle$ is generally unknown at time t_{cur} , a subset $\mathcal{I} \subseteq \mathbb{R}^2$ in which $\langle \hat{t}_{1,\text{in}}, \hat{t}_{1,\text{out}} \rangle$ must lie can always be obtained. Therefore, we can use this uncertainty set to characterize the *situation information*

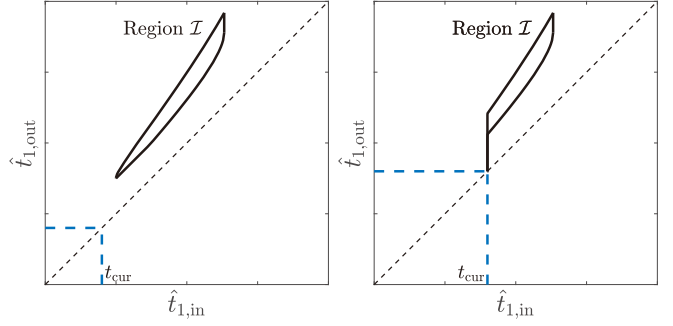


Fig. 4: The uncertainty set \mathcal{I} calculated by Proposition 1 at different t_{cur} based on the same observation.

obtained by s_0 at t_{cur} . Specifically, if nothing is known about s_1 at t_{cur} , we can let

$$\mathcal{I} = \left\{ \langle \hat{t}_{1,\text{in}}, \hat{t}_{1,\text{out}} \rangle \left| \begin{array}{l} \hat{t}_{1,\text{in}} = \max\{t_{1,\text{in}}, t_{\text{cur}}\} \\ \hat{t}_{1,\text{out}} = \max\{t_{1,\text{out}}, t_{\text{cur}}\} \\ t_{1,\text{out}} \leq B \\ 0 \leq t_{1,\text{in}} \leq t_{1,\text{out}} - L_1/v_M \end{array} \right. \right\}. \quad (16)$$

When some information on s_1 is available, \mathcal{I} can be narrowed to a subset of (16), and different types of information can be fused by intersecting their respective subsets.

In the next two propositions, we specifically calculate and characterize the uncertainty set \mathcal{I} for the scenario where the *accurate state* of s_1 at time $t_{\text{obs}} \leq t_{\text{cur}}$ is observed. Note that this scenario allows a positive age of information and is common in various practical scenarios.

Proposition 1: Suppose $\mathbf{x}_1(t_{\text{obs}}) = \mathbf{x}_*$ is observed at time t_{obs} , where $t_{\text{obs}} \leq t_{\text{cur}}$. Then for any trajectory of s_1 according with the observation, $\langle \hat{t}_{1,\text{in}}, \hat{t}_{1,\text{out}} \rangle$ must lie in \mathcal{I} , where \mathcal{I} is defined as follows.

(i) If $p_1(t_{\text{obs}}) \leq 0$, then

$$\mathcal{I} = \left\{ \langle \hat{t}_{1,\text{in}}, \hat{t}_{1,\text{out}} \rangle \left| \begin{array}{l} \text{Conditions in (16)} \\ t_{1,\text{in}}^{\sigma_A} \leq t_{1,\text{in}} \leq t_{1,\text{in}}^{\sigma_D} \\ t_{1,\text{out}}^{\sigma_{DA}(t_{1,\text{in}})} \leq t_{1,\text{out}} \leq t_{1,\text{out}}^{\sigma_{AD}(t_{1,\text{in}})} \end{array} \right. \right\} \quad (17)$$

where $\sigma_A, \sigma_D \in \Sigma_1(\mathbf{x}_*; t_{\text{obs}})$ are the ACC trajectory and the DEC trajectory on $[t_{\text{obs}}, +\infty)$, respectively; for any t_* , $\sigma_{DA}(t_*), \sigma_{AD}(t_*) \in \Sigma_1(\mathbf{x}_*; t_{\text{obs}})$ are the DEC-ACC trajectory and the ACC-DEC trajectory on $[t_{\text{obs}}, +\infty)$ satisfying $t_{1,\text{in}}^{\sigma_{DA}(t_*)} = t_{1,\text{in}}^{\sigma_{AD}(t_*)} = t_*$, respectively.⁴

(ii) If $0 < p_1(t_{\text{obs}}) < L_1$, then

$$\mathcal{I} = \left\{ \langle \hat{t}_{1,\text{in}}, \hat{t}_{1,\text{out}} \rangle \left| \begin{array}{l} \text{Conditions in (16)} \\ t_{1,\text{in}} \leq t_{\text{cur}} \\ t_{1,\text{out}}^{\sigma_A} \leq t_{1,\text{out}} \leq t_{1,\text{out}}^{\sigma_D} \end{array} \right. \right\} \quad (18)$$

where $\sigma_A, \sigma_D \in \Sigma_1(\mathbf{x}_*; t_{\text{obs}})$ are the ACC trajectory and the DEC trajectory on $[t_{\text{obs}}, +\infty)$, respectively.

(iii) If $p_1(t_{\text{obs}}) \geq L_1$, then $\mathcal{I} = \{\langle t_{\text{cur}}, t_{\text{cur}} \rangle\}$.

Proof: See Appendix B. \square

⁴For the last inequality in (17), if the trajectory $\sigma_{DA}(t_{1,\text{in}})$ or $\sigma_{AD}(t_{1,\text{in}})$ does not exist for some $t_{1,\text{in}}$, we omit the corresponding side of the inequality.

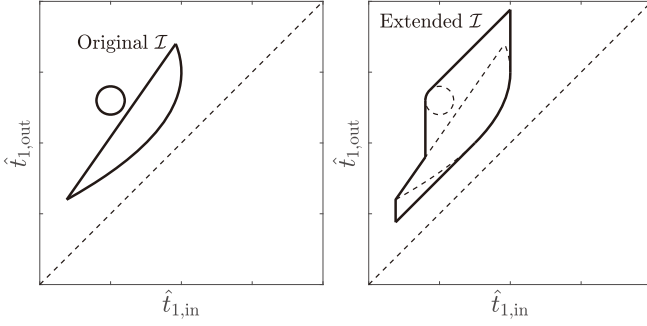


Fig. 5: An extension of a general uncertainty set \mathcal{I} which makes it satisfy Assumption 2.

Proposition 2: Let \mathcal{I} be the set defined in Proposition 1. Then \mathcal{I} is closed and simply connected, and $\mathcal{I} \cap \{\hat{t}_{1,\text{in}} = t_*\}$ is either empty or a closed interval for any t_* . Furthermore, if $\mathcal{I} \cap \{\hat{t}_{1,\text{in}} = t_*\}$ is non-empty, let

$$\hat{t}_{1,\text{out}}(t_*) \triangleq \min(\mathcal{I} \cap \{\hat{t}_{1,\text{in}} = t_*\}) \quad (19)$$

$$\overline{\hat{t}_{1,\text{out}}}(t_*) \triangleq \max(\mathcal{I} \cap \{\hat{t}_{1,\text{in}} = t_*\}). \quad (20)$$

Then both $\hat{t}_{1,\text{out}}(t_*) - t_*$ and $\overline{\hat{t}_{1,\text{out}}}(t_*) - t_*$ are positive and non-decreasing functions with respect to t_* .

Proof: See Appendix C. \square

Fig. 4 provides two examples of the uncertainty set \mathcal{I} calculated by Proposition 1, from which the properties in Proposition 2 can be intuitively checked. The last result in Proposition 2 implies that $\hat{t}_{1,\text{out}} - \hat{t}_{1,\text{in}}$ is generally positively correlated with $\hat{t}_{1,\text{in}}$. This result accords with intuition since a smaller $\hat{t}_{1,\text{in}}$ often corresponds to a trajectory with more acceleration, which can also lead to a smaller $\hat{t}_{1,\text{out}} - \hat{t}_{1,\text{in}}$.

The results in Proposition 2 can provide much convenience for the further analyses, while it is based on the scenario of accurate state observation. Therefore, we make the following assumption for the general case.

Assumption 2: $\mathcal{I} \subseteq \mathbb{R}^2$ always satisfies Proposition 2.

It is easy to check that besides the case of accurate state information, the maximum uncertainty set given in (16) also satisfies Assumption 2. For a general uncertainty set to which Assumption 2 may not hold, set extensions can be performed to make it satisfy the assumption. An example of the extension is illustrated in Fig. 5.

B. State Value Function

In this subsection, we still consider a fixed time t_{cur} with $p_0(t_{\text{cur}}) \leq 0$, and propose a state value function for s_0 under a given situation information \mathcal{I} .

We start from the scheduling cost defined in (9). We have shown in (14) that $\langle \hat{t}_{1,\text{in}}, \hat{t}_{1,\text{out}} \rangle$ can be used to replace $\langle t_{1,\text{in}}, t_{1,\text{out}} \rangle$. However, note that $\langle \hat{t}_{1,\text{in}}, \hat{t}_{1,\text{out}} \rangle$ is unknown, and based on the obtained situation information, s_0 can only

access the following function

$$C_{\max}(\sigma_0; \mathcal{I}) \triangleq \max_{\langle \hat{t}_{1,\text{in}}, \hat{t}_{1,\text{out}} \rangle \in \mathcal{I}} C(\sigma_0; \hat{t}_{1,\text{in}}, \hat{t}_{1,\text{out}}) = \begin{cases} v_M t_{0,\text{in}}^{\sigma_0} + \frac{1}{2a_{0,M}} (v_M - v_0^{\sigma_0}(t_{0,\text{in}}^{\sigma_0}))^2, \\ \text{if } (t_{0,\text{in}}^{\sigma_0}, t_{0,\text{out}}^{\sigma_0}) \cap \mathcal{W}(\mathcal{I}) = \emptyset; \\ +\infty, \text{ otherwise} \end{cases} \quad (21)$$

where

$$\mathcal{W}(\mathcal{I}) \triangleq \bigcup_{\langle \hat{t}_{1,\text{in}}, \hat{t}_{1,\text{out}} \rangle \in \mathcal{I}} (\hat{t}_{1,\text{in}}, \hat{t}_{1,\text{out}}). \quad (22)$$

Specifically, we refer to the condition

$$(t_{0,\text{in}}, t_{0,\text{out}}) \cap \mathcal{W}(\mathcal{I}) = \emptyset \quad (23)$$

as the *robust safety condition* under the situation information \mathcal{I} to make a distinction with the safety condition (7).

A further observation on (21) is that the time-related part $v_M t_{0,\text{in}}^{\sigma_0}$ contains two constant and ineliminable components for a fixed t_{cur} and \mathcal{I} . Specifically, s_0 is not able to occupy the resource in $[0, t_{\text{cur}}]$ due to causality, and is also not able to start the occupation during $\mathcal{W}(\mathcal{I})$ due to the robust safety condition. Therefore, for the purpose of performing state evaluation, we drop these uncontrollable components and define the *manageable cost* as follows.

Definition 4 (Manageable Cost): Let \mathcal{I} be the obtained situation information at time t_{cur} . Then for a given trajectory σ_0 of s_0 , the manageable cost is defined by

$$C^*(\sigma_0; t_{\text{cur}}, \mathcal{I}) \triangleq \begin{cases} v_M \delta(\sigma_0; t_{\text{cur}}, \mathcal{I}) + \frac{1}{2a_{0,M}} (v_M - v_0^{\sigma_0}(t_{0,\text{in}}^{\sigma_0}))^2, \\ \text{if } (t_{0,\text{in}}^{\sigma_0}, t_{0,\text{out}}^{\sigma_0}) \cap \mathcal{W}(\mathcal{I}) = \emptyset; \\ +\infty, \text{ otherwise} \end{cases} \quad (24)$$

where

$$\delta(\sigma_0; t_{\text{cur}}, \mathcal{I}) \triangleq \mu[(t_{\text{cur}}, t_{0,\text{in}}^{\sigma_0}) \setminus \mathcal{W}(\mathcal{I})]. \quad (25)$$

To characterize the preference of different states, we introduce the concept of *state value function*, whose name is borrowed from the reinforcement learning researches. Specifically, for a given state, its value is defined by minimizing the manageable cost over all trajectories of s_0 starting from this state, as shown in the next definition.

Definition 5 (State Value Function): Let \mathcal{I} be the obtained situation information at time t_{cur} . Then the state value function of s_0 is defined by

$$V(\mathbf{x}; t_{\text{cur}}, \mathcal{I}) \triangleq \min_{\sigma_0 \in \Sigma_0(\mathbf{x}; t_{\text{cur}})} C^*(\sigma_0; t_{\text{cur}}, \mathcal{I}). \quad (26)$$

Intuitively, states with smaller V are more appealing based on the situation information \mathcal{I} , since they have a potential to result in a smaller manageable cost C^* . However, (26) is defined by a minimization problem and is indirect to calculate. Thus, we provide the next proposition characterizing a solution of the minimization in (26). Specifically, the problem of calculating the state value function is transformed to calculating the manageable cost for a specific DEC-ACC trajectory.

Proposition 3: Let Λ be the set of DEC-ACC trajectories on $[t_{\text{cur}}, +\infty)$ in $\Sigma_0(\mathbf{x}; t_{\text{cur}})$ satisfying the robust safety condition (23). If $\Lambda \neq \emptyset$, let $\sigma^* \triangleq \arg \min_{\sigma \in \Lambda} t_D^\sigma$.⁵ Then

$$V(\mathbf{x}; t_{\text{cur}}, \mathcal{I}) = \begin{cases} C^*(\sigma^*; t_{\text{cur}}, \mathcal{I}), & \text{if } \Lambda \neq \emptyset; \\ +\infty, & \text{otherwise.} \end{cases} \quad (27)$$

Furthermore, if $\Lambda \neq \emptyset$, then σ^* has the smallest $t_{0,\text{in}}$ and the largest $v_0(t_{0,\text{in}})$ within all trajectories in $\Sigma_0(\mathbf{x}; t_{\text{cur}})$ satisfying (23).

Proof: See Appendix D. \square

IV. MINIMAX CONTROL POLICY

In this section, we establish the framework of the minimax control policy for the agent s_0 , present the safety guarantee and provide algorithms for the implementation of the policy.

A. Policy Statement and Safety Guarantee

Recall that decisions are made at times $\{t_k \mid k \geq 0\}$ where $t_0 = 0$ and $t_k < t_{k+1}$ for any $k \geq 0$. Specifically, we only need to focus on the one-step decision at t_k , when the state $\mathbf{x}_0(t_k) = \langle p_0(t_k), v_0(t_k) \rangle$ has been fixed with $p_0(t_k) \leq 0$, and s_0 needs to determine the trajectory during the time interval $[t_k, t_{k+1}]$ based on the situation information \mathcal{I}_k .

Firstly, s_0 needs to determine whether there exists a trajectory $\sigma \in \Sigma_0(\mathbf{x}_0(t_k); t_k)$ allowing it to safely access the resource during the upcoming interval $[t_k, t_{k+1}]$. In other words, σ should simultaneously satisfy

$$(t_{0,\text{in}}^\sigma, t_{0,\text{out}}^\sigma) \cap \mathcal{W}(\mathcal{I}_k) = \emptyset, \quad t_{0,\text{in}}^\sigma \leq t_{k+1}. \quad (28)$$

The next proposition characterizes an equivalent condition for the existence of such a trajectory which is easier to verify.

Proposition 4: Let Λ be the set of DEC-ACC trajectories on $[t_k, +\infty)$ in $\Sigma_0(\mathbf{x}_0(t_k); t_k)$ satisfying $(t_{0,\text{in}}, t_{0,\text{out}}) \cap \mathcal{W}(\mathcal{I}_k) = \emptyset$. If $\Lambda \neq \emptyset$, let $\sigma^* \triangleq \arg \min_{\sigma \in \Lambda} t_D^\sigma$. Then a trajectory $\sigma \in \Sigma_0(\mathbf{x}_0(t_k); t_k)$ satisfying (28) exists if and only if

$$\Lambda \neq \emptyset, \quad t_{0,\text{in}}^{\sigma^*} \leq t_{k+1}. \quad (29)$$

Proof: If σ^* satisfying (29) exists, then it can serve as the σ we are finding. Conversely, if the trajectory σ satisfying (28) exists, then $V(\mathbf{x}_0(t_k); t_k, \mathcal{I}_k)$ is finite. By Proposition 3, $\Lambda \neq \emptyset$ and we have $t_{0,\text{in}}^{\sigma^*} \leq t_{0,\text{in}}^\sigma \leq t_{k+1}$, which completes the proof. \square

According to Proposition 4, if (29) holds, then s_0 is able to obtain the resource before t_{k+1} . In this case, σ^* is exactly the trajectory which can result in the smallest manageable cost by Proposition 3, and thus s_0 should follow σ^* during $[t_k, t_{k+1}]$. On the contrary, if (29) does not hold, we divide the decision of s_0 at t_k into two steps. First, a target state $\mathbf{x}_{\text{tar}} = \langle p_{\text{tar}}, v_{\text{tar}} \rangle$ is determined which satisfies $p_{\text{tar}} \leq 0$, and second, a trajectory $\sigma \in \Sigma_0(\mathbf{x}_0(t_k); t_k)$ on the interval $[t_k, t_{k+1}]$ is generated which satisfies

$$\mathbf{x}_0^\sigma(t_{k+1}) = \mathbf{x}_{\text{tar}}. \quad (30)$$

⁵It is easy to check that $\{t_D^\sigma \mid \sigma \in \Lambda\}$ is closed and has a lower bound t_{cur} . Therefore, σ^* must exist.

Algorithm 1 The decision of s_0 at time t_k

Input: $L_0, v_M, a_{0,m}, a_{0,M}, \mathbf{x}_0(t_k), \mathcal{I}_k$.

Output: Trajectory on $[t_k, t_{k+1}]$.

- 1: Find σ^* by Proposition 3.
 - 2: **if** (29) holds **then**
 - 3: Return σ^* .
 - 4: **else**
 - 5: Solve (34) to obtain $\mathbf{x}_{\text{tar}} \in \mathcal{F}_k$.
 - 6: Return an arbitrary trajectory $\sigma \in \Sigma_0(\mathbf{x}_0(t_k); t_k)$ on $[t_k, t_{k+1}]$ satisfying (30).
 - 7: **end if**
-

Let \mathcal{F}_k be the set of target states such that the corresponding trajectory σ satisfying (30) exists, i.e.,

$$\mathcal{F}_k \triangleq \left\{ \mathbf{x}_0^\sigma(t_{k+1}) \left| \begin{array}{l} \sigma \in \Sigma_0(\mathbf{x}_0(t_k); t_k) \\ p_0^\sigma(t_{k+1}) \leq 0 \end{array} \right. \right\}. \quad (31)$$

Then we can find that as long as $\mathbf{x}_{\text{tar}} \in \mathcal{F}_k$ is fixed, the choice of the specific trajectory σ in the second step does not make any difference for subsequent decisions. Therefore, we focus on the first step of the decision, which aims to determine which target state $\mathbf{x}_{\text{tar}} \in \mathcal{F}_k$ is the most preferred for the time t_{k+1} .

Recall that the state value function $V(\mathbf{x}_{\text{tar}}; t_{k+1}, \mathcal{I}_{k+1})$ proposed in Definition 5 is a natural criterion to evaluate the preference of different target states. However, note that s_0 have no access to \mathcal{I}_{k+1} at the decision time t_k . Therefore, a *minimax framework* is adopted for the decision, where we take into account all possible \mathcal{I}_{k+1} and optimize the worst-case performance. Specifically, note that since \mathcal{I}_{k+1} must be consistent with the current information \mathcal{I}_k , it must lie in

$$\mathcal{J}_k \triangleq \left\{ \mathcal{I}_{k+1} \left| \begin{array}{l} \mathcal{I}_{k+1} \subseteq \max\{t_{k+1}, \mathcal{I}_k\} \\ \text{satisfying Assumption 2} \end{array} \right. \right\} \quad (32)$$

where

$$\begin{aligned} & \max\{t_{k+1}, \mathcal{I}_k\} \\ & \triangleq \left\{ \left\langle \begin{array}{l} \max\{t_{k+1}, \hat{t}_{1,\text{in}}\}, \\ \max\{t_{k+1}, \hat{t}_{1,\text{out}}\} \end{array} \right\rangle \left| \langle \hat{t}_{1,\text{in}}, \hat{t}_{1,\text{out}} \rangle \in \mathcal{I}_k \right. \right\}. \end{aligned} \quad (33)$$

Then the decision is made by

$$\arg \min_{\mathbf{x}_{\text{tar}} \in \mathcal{F}_k} \max_{\mathcal{I}_{k+1} \in \mathcal{J}_k} V(\mathbf{x}_{\text{tar}}; t_{k+1}, \mathcal{I}_{k+1}). \quad (34)$$

The full procedure of the proposed control policy at the decision time t_k is concluded in Algorithm 1.

Now we analyze the safety of the policy; in other words, we need to show the output trajectory of the proposed policy satisfies the safety condition (7). Recall (24) and (26) that for a state \mathbf{x} at time t_k , $V(\mathbf{x}; t_k, \mathcal{I}_k) < +\infty$ implies that there exists a trajectory in $\Sigma_0(\mathbf{x}; t_k)$ satisfying the robust safety condition, which intuitively means that the state \mathbf{x} has the potential of maintaining safety in the future. Therefore, the safety of the policy can be verified by showing that $V(\mathbf{x}_0(t_k); t_k, \mathcal{I}_k) < +\infty$ always holds at each time t_k , which can be proved by induction. Specifically, we have the following theorem.

Theorem 1: Let $\{t_k \mid k \geq 0\}$ be a set of decision times of s_0 with $t_0 = 0$ and $t_k < t_{k+1}$ for any $k \geq 0$. At each decision

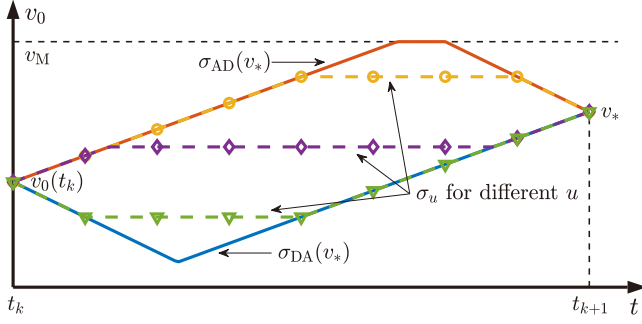


Fig. 6: The illustration of the parameterized trajectory family $\{\sigma_u\}$ defined by (36) deforming $\sigma_{DA}(v_*)$ into $\sigma_{AD}(v_*)$, where $v_0^{u_0}(t_{k+1}) = v_*$ always holds.

time, s_0 makes decision according to Algorithm 1. Then the trajectory of s_0 satisfies the safety condition (7).

Proof: See Appendix E. \square

Finally, we provide a remark on the proposed framework.

Remark 1: Note that this article focuses on the perspective of one agent instead of the entire system, and agents are not assumed to be cooperative. Therefore, if the two agents both follow the proposed policy, deadlocks may occur since neither of them dare to occupy the resource without knowing how the other agent will react. To eliminate the deadlock, extra mechanisms need to be introduced such as directly specifying the order by a central node when both agents have stopped near the resource.

The next two subsections provide further characterizations and algorithms on (34).

B. Range of Feasible Target States

In this subsection, we provide another descriptive characterization of the set \mathcal{F}_k defined in (31), which serves as the objective space of the optimization problem (34).

Proposition 5: Fix the state $\mathbf{x}_0(t_k)$. Then

$$\mathcal{F}_k = \left\{ \langle p, v \rangle \left| \begin{array}{l} p \leq 0 \\ v_0^{\sigma_D}(t_{k+1}) \leq v \leq v_0^{\sigma_A}(t_{k+1}) \\ p_0^{\sigma_{DA}(v)}(t_{k+1}) \leq p \leq p_0^{\sigma_{AD}(v)}(t_{k+1}) \end{array} \right. \right\} \quad (35)$$

where $\sigma_A, \sigma_D \in \Sigma_0(\mathbf{x}_0(t_k); t_k)$ are the ACC trajectory and the DEC trajectory on $[t_k, t_{k+1}]$, respectively; for a given v , $\sigma_{DA}(v), \sigma_{AD}(v) \in \Sigma_0(\mathbf{x}_0(t_k); t_k)$ are the DEC-ACC trajectory and the ACC-DEC trajectory on $[t_k, t_{k+1}]$ satisfying $v_0^{\sigma_{DA}(v)}(t_{k+1}) = v_0^{\sigma_{AD}(v)}(t_{k+1}) = v$, respectively.⁶

Proof: For any $\mathbf{x}_0^g(t_{k+1}) \in \mathcal{F}_k$, we can check that it also belongs to the right-hand side of (35). Conversely, for any $\mathbf{x}_* = \langle p_*, v_* \rangle$ in the right-hand side of (35), we need to find a trajectory $\sigma \in \Sigma_0(\mathbf{x}_0(t_k); t_k)$ with $\mathbf{x}_0^g(t_{k+1}) = \mathbf{x}_*$. To this end, we construct a one-dimensional parameterized family $\{\sigma_u\} \subseteq \Sigma_0(\mathbf{x}_0(t_k); t_k)$ of trajectories which continuously deforms $\sigma_{DA}(v_*)$ into $\sigma_{AD}(v_*)$ with $v_0^{u_0}(t_{k+1}) = v_*$ always holds. For example, we can let

$$v_0^u(t) = \max \left\{ \min \{u, v_0^{\sigma_{AD}(v_*)}(t)\}, v_0^{\sigma_{DA}(v_*)}(t) \right\} \quad (36)$$

⁶For $v \in [v_0^{\sigma_D}(t_{k+1}), v_0^{\sigma_A}(t_{k+1})]$, the existence of $\sigma_{DA}(v)$ (or $\sigma_{AD}(v)$) comes from the continuity of $v_0^g(t_{k+1})$ with respect to t_D^g (or t_A^g), which is discussed in Lemma 2 in Appendix A.

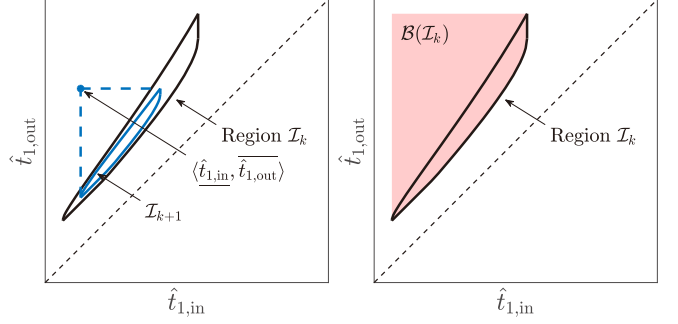


Fig. 7: The left subfigure shows the calculation of $\overline{\langle \hat{t}_{1,\text{in}}, \hat{t}_{1,\text{out}} \rangle}$ for a specific $\mathcal{I}_{k+1} \in \mathcal{J}_k$, and the right subfigure illustrates the set $\mathcal{B}(\mathcal{I}_k)$ defined in Proposition 6 which contains all possible $\overline{\langle \hat{t}_{1,\text{in}}, \hat{t}_{1,\text{out}} \rangle}$.

for all $t \in [t_k, t_{k+1}]$, and Fig. 6 provides the illustration of this example on the (v_0, t) -plane. Note that by the continuity, the family $\{\sigma_u\}$ must include a trajectory σ_{u_0} satisfying $p_0^{\sigma_{u_0}}(t_{k+1}) = p_*$. This completes the proof. \square

Note that compared with the original definition (31) of \mathcal{F}_k , (35) is more descriptive since it directly characterizes the inequalities on p and v . Furthermore, the proof of Proposition 5 actually provides a method to find a trajectory on $[t_k, t_{k+1}]$ after given the target state $\mathbf{x}_{\text{tar}} \in \mathcal{F}_k$, which can be applied in the Line 6 of Algorithm 1.

C. Calculating the Maximum

In this subsection, we focus on calculating the objective function of the minimization in (34), i.e.,

$$V_{\max}(\mathbf{x}_{\text{tar}}; t_{k+1}, \mathcal{I}_k) \triangleq \max_{\mathcal{I}_{k+1} \in \mathcal{J}_k} V(\mathbf{x}_{\text{tar}}; t_{k+1}, \mathcal{I}_{k+1}) \quad (37)$$

which itself is represented by another optimization problem. For simplicity of notations, we omit \mathbf{x}_{tar} and t_{k+1} which are always fixed in this subsection, and write

$$V_{\max}(\mathcal{I}_k) \triangleq \max_{\mathcal{I}_{k+1} \in \mathcal{J}_k} V(\mathcal{I}_{k+1}). \quad (38)$$

According to Definitions 4 and 5, the state value function $V(\mathcal{I}_{k+1})$ only depends on $\mathcal{W}(\mathcal{I}_{k+1})$, where the definition of $\mathcal{W}(\cdot)$ is provided in (22). By utilizing Assumption 2, for any $\mathcal{I}_{k+1} \in \mathcal{J}_k$, we have

$$\mathcal{W}(\mathcal{I}_{k+1}) = \overline{\langle \hat{t}_{1,\text{in}}, \hat{t}_{1,\text{out}} \rangle} \quad (39)$$

where

$$\hat{t}_{1,\text{in}} \triangleq \min \{ \hat{t}_{1,\text{in}} \mid \exists \hat{t}_{1,\text{out}}, \langle \hat{t}_{1,\text{in}}, \hat{t}_{1,\text{out}} \rangle \in \mathcal{I}_{k+1} \} \quad (40)$$

$$\hat{t}_{1,\text{out}} \triangleq \max \{ \hat{t}_{1,\text{out}} \mid \exists \hat{t}_{1,\text{in}}, \langle \hat{t}_{1,\text{in}}, \hat{t}_{1,\text{out}} \rangle \in \mathcal{I}_{k+1} \}. \quad (41)$$

The calculation of $\hat{t}_{1,\text{in}}$ and $\hat{t}_{1,\text{out}}$ is illustrated in the left subfigure in Fig. 7. Therefore, we can use the alternative notation $V(\hat{t}_{1,\text{in}}, \hat{t}_{1,\text{out}})$ for $V(\mathcal{I}_{k+1})$.

Now we characterize the range of the pair $\overline{\langle \hat{t}_{1,\text{in}}, \hat{t}_{1,\text{out}} \rangle}$ in the next proposition.

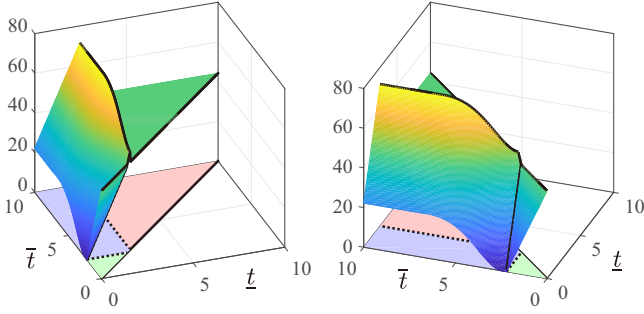


Fig. 8: The graph of the function $V(\underline{t}, \bar{t})$ from two angles. Parameters $v_M = 20$, $a_{0,m} = 4$, $a_{0,M} = 3$, $L_0 = 5$, $p_{\text{tar}} = -40$, and $v_{\text{tar}} = 15$. The domain division is shown on the ground plane that \mathcal{D}_1 is colored in red, \mathcal{D}_2 in green, and \mathcal{D}_3 in blue. The boundaries of the three sub-regions are also displayed on the graph of the function by black curves.

Proposition 6: For a given situation information \mathcal{I}_k , the corresponding range of $\langle \hat{t}_{1,\text{in}}, \hat{t}_{1,\text{out}} \rangle$ is

$$\mathcal{B}(\mathcal{I}_k) \triangleq \left\{ \left\langle \min\{\hat{t}_{1,\text{in}}^{(1)}, \hat{t}_{1,\text{in}}^{(2)}\}, \max\{\hat{t}_{1,\text{out}}^{(1)}, \hat{t}_{1,\text{out}}^{(2)}\} \right\rangle \left| \begin{array}{l} \langle \hat{t}_{1,\text{in}}^{(1)}, \hat{t}_{1,\text{out}}^{(1)} \rangle, \langle \hat{t}_{1,\text{in}}^{(2)}, \hat{t}_{1,\text{out}}^{(2)} \rangle \in \mathcal{I}_k \end{array} \right. \right\}. \quad (42)$$

Proof: See Appendix F. \square

The set $\mathcal{B}(\mathcal{I}_k)$ is shown in the right subfigure in Fig. 7. According to Proposition 6, our goal of calculating (38) is transformed to

$$V_{\max}(\mathcal{I}_k) = \max_{(\underline{t}, \bar{t}) \in \mathcal{B}(\mathcal{I}_k)} V(\underline{t}, \bar{t}). \quad (43)$$

Note that here we regard \underline{t} and \bar{t} as two free variables. Before solving (43), we first show another property of the optimization range $\mathcal{B}(\mathcal{I}_k)$.

Proposition 7: Let $\langle \underline{t}^{(1)}, \bar{t}^{(1)} \rangle, \langle \underline{t}^{(2)}, \bar{t}^{(2)} \rangle \in \mathcal{B}(\mathcal{I}_k)$. Then the following four pairs are also in $\mathcal{B}(\mathcal{I}_k)$:

$$\langle \underline{t}^{(1)}, \max\{\bar{t}^{(1)}, \bar{t}^{(2)}\} \rangle, \quad \langle \underline{t}^{(2)}, \max\{\bar{t}^{(1)}, \bar{t}^{(2)}\} \rangle, \quad (44)$$

$$\langle \min\{\underline{t}^{(1)}, \underline{t}^{(2)}\}, \bar{t}^{(1)} \rangle, \quad \langle \min\{\underline{t}^{(1)}, \underline{t}^{(2)}\}, \bar{t}^{(2)} \rangle. \quad (45)$$

Proof: See Appendix G. \square

Now we analyze the monotonicity of the function $V(\underline{t}, \bar{t})$, which is defined on the domain

$$\mathcal{D} \triangleq \{(\underline{t}, \bar{t}) \mid t_{k+1} \leq \underline{t} \leq \bar{t} \leq B\}. \quad (46)$$

To start, we divide this domain into the following three parts⁷

$$\mathcal{D}_1 \triangleq \{(\underline{t}, \bar{t}) \mid t_{0,\text{out}}^{\sigma_A} \leq \underline{t} \leq \bar{t} \leq B\} \quad (47)$$

$$\mathcal{D}_2 \triangleq \{(\underline{t}, \bar{t}) \mid t_{k+1} \leq \underline{t} \leq \bar{t} \leq t_{0,\text{in}}^{\sigma_A}\} \quad (48)$$

$$\mathcal{D}_3 \triangleq \left\{ (\underline{t}, \bar{t}) \left| \begin{array}{l} t_{k+1} \leq \underline{t} \leq t_{0,\text{out}}^{\sigma_A} \\ t_{0,\text{in}}^{\sigma_A} \leq \bar{t} \leq B \\ \underline{t} \leq \bar{t} \end{array} \right. \right\} \quad (49)$$

⁷Although we use the word “divide”, we set all three sub-regions closed for convenience, and thus their mutual intersections are one-dimensional line segments instead of the empty set.

Algorithm 2 Solving the maximization in (38)

Input: $L_0, v_M, a_{0,m}, a_{0,M}, \mathbf{x}_{\text{tar}}, \mathcal{I}_k$.

Output: $V_{\max}(\mathcal{I}_k)$.

1: Find $\mathcal{B}(\mathcal{I}_k)$ by Proposition 6.

2: Separately maximizing $V(\underline{t}, \bar{t})$ in the three sub-regions by Proposition 8, and return the one with the largest value.

in which $\sigma_A \in \Sigma_0(\mathbf{x}_{\text{tar}}; t_{k+1})$ is the ACC trajectory on $[t_{k+1}, +\infty)$. The next theorem analyzes the monotonicity of $V(\underline{t}, \bar{t})$ on the three sub-regions defined above.

Theorem 2: For a given state \mathbf{x}_{tar} of s_0 at time t_{k+1} , the function $V(\underline{t}, \bar{t})$ satisfies the following properties.

- (i) V is constant on \mathcal{D}_1 .
- (ii) V only depends on $\bar{t} - \underline{t}$ on \mathcal{D}_2 , and decreases with $\bar{t} - \underline{t}$. Furthermore, the value of V on \mathcal{D}_2 is always no larger than its value on \mathcal{D}_1 .
- (iii) V is non-decreasing with respect to both \underline{t} and \bar{t} on \mathcal{D}_3 .

Proof: See Appendix H. \square

Fig. 8 provides the graph of the function $V(\underline{t}, \bar{t})$ from two angles under certain parameters, which supports our results in Theorem 2. Based on the theorem, solving the optimization problem (43) becomes straightforward, and the solution is presented in the next proposition.

Proposition 8: Fix the state \mathbf{x}_{tar} of s_0 at time t_{k+1} and the situation information \mathcal{I}_k at time t_k .

- (i) If $\mathcal{B}(\mathcal{I}_k) \cap \mathcal{D}_1$ is non-empty, then the maximum value of $V(\underline{t}, \bar{t})$ in $\mathcal{B}(\mathcal{I}_k) \cap \mathcal{D}_1$ is obtained at any point in $\mathcal{B}(\mathcal{I}_k) \cap \mathcal{D}_1$.
- (ii) If $\mathcal{B}(\mathcal{I}_k) \cap \mathcal{D}_2$ is non-empty, then the maximum value of $V(\underline{t}, \bar{t})$ in $\mathcal{B}(\mathcal{I}_k) \cap \mathcal{D}_2$ is obtained at

$$\left\langle \min_{(\underline{t}, \bar{t}) \in \mathcal{B}(\mathcal{I}_k) \cap \mathcal{D}_2} \underline{t}, \min_{(\underline{t}, \bar{t}) \in \mathcal{B}(\mathcal{I}_k) \cap \mathcal{D}_2} \bar{t} \right\rangle. \quad (50)$$

- (iii) If $\mathcal{B}(\mathcal{I}_k) \cap \mathcal{D}_3$ is non-empty, then the maximum value of $V(\underline{t}, \bar{t})$ in $\mathcal{B}(\mathcal{I}_k) \cap \mathcal{D}_3$ is obtained at

$$\left\langle \max_{(\underline{t}, \bar{t}) \in \mathcal{B}(\mathcal{I}_k) \cap \mathcal{D}_3} \underline{t}, \max_{(\underline{t}, \bar{t}) \in \mathcal{B}(\mathcal{I}_k) \cap \mathcal{D}_3} \bar{t} \right\rangle. \quad (51)$$

Proof: See Appendix I. \square

According to Proposition 8, we only need to calculate at most three values of $V(\underline{t}, \bar{t})$ to solve (43), or equivalently, (38). This number can be further reduced into two, since if $\mathcal{B}(\mathcal{I}_k)$ has non-empty intersections with all three sub-regions, then $\mathcal{B}(\mathcal{I}_k) \cap \mathcal{D}_2$ can be neglected by Theorem 2(ii).

Remark 2: If $\underline{t} = t_{k+1}$ for all $(\underline{t}, \bar{t}) \in \mathcal{B}(\mathcal{I}_k)$, then by Proposition 8, the maximum value of $V(\underline{t}, \bar{t})$ in $\mathcal{B}(\mathcal{I}_k)$ can only be obtained at one of the two endpoints, i.e.,

$$\left\langle t_{k+1}, \max_{(t_{k+1}, \bar{t}) \in \mathcal{B}(\mathcal{I}_k)} \bar{t} \right\rangle \text{ or } \left\langle t_{k+1}, \min_{(t_{k+1}, \bar{t}) \in \mathcal{B}(\mathcal{I}_k)} \bar{t} \right\rangle. \quad (52)$$

This special case was presented in our previous work [45].

In summary, the algorithm of calculating $V_{\max}(\mathcal{I}_k)$ is concluded in Algorithm 2.

V. DISCUSSIONS

In this section, we provide intuitions and several generalizations on the proposed minimax scheduling framework.

A. Intuitions

In this subsection, we provide intuitive interpretations on the scheduling problem with kinematic constraints and our minimax solution. Generally speaking, when facing another agent s_1 with unknown future trajectory, s_0 can choose from two *high-level decisions*:

- (i) trying to occupy the resource before s_1 , or
- (ii) choosing to start the occupation after s_1 .

Clearly, these two decisions will generate contradictory trajectory planning: under the first decision, s_0 tends to maintain the maximum velocity as long as the safety is ensured; under the second decision, s_0 should estimate $t_{1,\text{out}}$ in order to start the occupation as early and as fast as possible, and deceleration may be required in early stages.

However, due to the trajectory uncertainty of s_1 , s_0 cannot tell in advance which high-level decision is better. Intuitively, the first choice is clearly more efficient if the trial succeeds; however, if s_1 moves too fast, then the failed trial will result in a large “velocity cost”. In contrast, the second choice can reduce the “velocity cost”, while it may face a large “time cost” if s_1 moves too slow. Therefore, no matter which high-level decision is made, it may turn out to be inefficient.

To resolve this difficulty, our framework does not make the high-level decision in advance. Instead, the low-level trajectory planning is directly performed, by which the possibilities of both high-level choices are still preserved. Specifically, in each step, the tradeoff between acceleration and deceleration is obtained by optimizing the potential scheduling cost in the worst case, which includes both the “time cost” part and the “velocity cost” part. Therefore, it is reasonable for our minimax framework to have a robust scheduling performance.

B. Generalizations

In this subsection, we introduce some generalizations on the applicable scenarios of the proposed scheduling framework.

1) *Weakly Cooperative Agents*: Several types of weak cooperation between s_0 and s_1 can be introduced into the proposed framework.⁸ For example, if s_1 makes *promises* to s_0 on its velocity (or acceleration) constraint which is stricter than (1) (or (2)), then s_0 can correspondingly change the axis scaling of s_1 (or $a_{1,m}$ and $a_{1,M}$) in the calculation.

Another commonly-used weak cooperation scheme is determining the *resource occupation order* through communications. If s_0 has the priority, then it can ignore s_1 and follow the ACC trajectory. Otherwise, if s_1 has the priority, then s_0 should change the length of s_1 to $L_1 + \alpha$ and change any position observation $p_1(t_{\text{obs}})$ to $p_1(t_{\text{obs}}) + \alpha$ for a large enough α in its calculation.

2) *Regularity of Information Collection*: In our framework introduced above, we did not assume any regularity on the process of information collection. In other words, at a decision time t_k , the uncertainty set for the next decision time t_{k+1} can take any element in \mathcal{J}_k as defined in (32). However, a certain regularity can help us further narrow down the set \mathcal{J}_k . For example, if s_0 already knows at t_k that it will not

⁸By “weak”, we mean that s_0 and s_1 are still separately controlled.

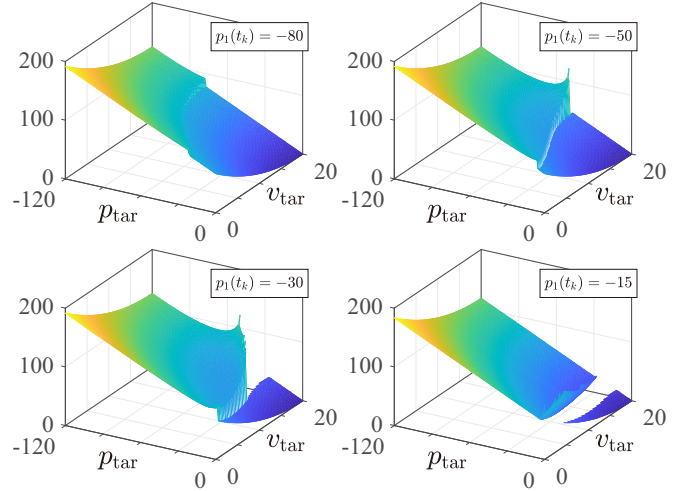


Fig. 9: The objective function $V_{\max}(\mathbf{x}_{\text{tar}}; t_{k+1}, \mathcal{I}_k)$. Parameters $v_M = 20$, $a_{0,m} = a_{1,m} = 4$, $a_{0,M} = a_{1,M} = 3$, $L_0 = L_1 = 5$, $v_1(t_k) = 15$, and $t_{k+1} - t_k = 0.01$. Regions with no value represent infinity.

obtain any new information at t_{k+1} ,⁹ then the maximum in (34) can be removed by taking $\mathcal{I}_{k+1} = \max\{t_{k+1}, \mathcal{I}_k\}$; in contrast, if s_0 is confident to make undelayed observations at all decision times,¹⁰ then \mathcal{I}_{k+1} must lie in a 2-dimensional subset of \mathcal{J}_k parameterized by the observations. Note that although the framework is always adaptable, the algorithm in Section IV-C needs to be re-developed case by case.

3) *Bounded Control Error*: Assume that there exist bounded control errors for the agent s_0 . In other words, when s_0 tries to control itself to the state \mathbf{x}_{tar} at time t_k , it will actually arrive at the state $\mathbf{x}_{\text{tar}} + \mathbf{n}$ at time t_{k+1} , where the unknown error \mathbf{n} is bounded. In this case, we can add a maximization over the control errors and change (34) to

$$\min_{\mathbf{x}_{\text{tar}} \in \mathcal{F}_k} \max_{\mathbf{n}} \max_{\mathcal{I}_{k+1} \in \mathcal{J}_k} V(\mathbf{x}_{\text{tar}} + \mathbf{n}; t_{k+1}, \mathcal{I}_{k+1}). \quad (53)$$

VI. NUMERICAL RESULTS

In this section, we provide numerical experiments to show the characteristics of the objective function, verify the performance of the proposed scheduling policy, and evaluate the effects of several parameters.

A. Objective Function V_{\max}

In this subsection, we numerically characterize the objective function $V_{\max}(\mathbf{x}_{\text{tar}}; t_{k+1}, \mathcal{I}_k)$ of the one-step decision (34) at time t_k , which is defined in (37). We assume that s_0 is able to observe $\mathbf{x}_1(t_k)$, based on which the situation information \mathcal{I}_k can be calculated by Proposition 1. Then the graph of $V_{\max}(\mathbf{x}_{\text{tar}}; t_{k+1}, \mathcal{I}_k)$ is shown in Fig. 9 with respect to $\mathbf{x}_{\text{tar}} = \langle p_{\text{tar}}, v_{\text{tar}} \rangle$ for four different values of $p_1(t_k)$.

⁹This can occur, for example, if s_0 can only make observations at a lower frequency than the decision making, and no observations can be made during $[t_k, t_{k+1}]$.

¹⁰This can occur, for example, if the observation frequency of s_0 is much higher than the decision frequency, and the observation delays are much lower than the dynamics of agents.

According to Fig. 9, the general trend of V_{\max} decreases with both p_{tar} and v_{tar} , which is intuitive since a state closer to the resource and with larger velocity is generally more appealing. However, the existence of s_1 makes the function discontinuous. Specifically, the right side of the transition has a lower value of V_{\max} , since this region corresponds to the case that s_0 is always able to occupy the resource *before* s_1 by the ACC trajectory. With $p_1(t_k)$ approaching zero, the transition moves right accordingly and the gap becomes larger, since the room for s_0 to make adjustment decreases.

B. Performance Comparison

In this subsection, we compare the output trajectory and the scheduling cost of the proposed policy with two other families of policies Queueing(d) and Following(d) for $d \geq 0$. Specifically,¹¹

- Queueing(d) is the policy in which s_0 moves with the maximum possible acceleration which can lead to the state $\langle p_0, v_0 \rangle = \langle -d, 0 \rangle$ before it finds an ACC trajectory ensuring robust safety. Mathematically, $a_0(t) = a_{0,A}(t)$ if $\sigma_{0,A}$ satisfies (23) or if $p_0(t) + \frac{v_0^2(t)}{2a_{0,m}} < -d$ holds; otherwise, $a_0(t) = a_{0,D}(t)$.
- Following(d) is the policy in which s_0 moves with the maximum possible acceleration which can ensure $p_0(t) < p_1(t) - L_1 - d$ for all t in the future before it finds an ACC trajectory ensuring robust safety. Mathematically, $a_0(t) = a_{0,A}(t)$ if $\sigma_{0,A}$ satisfies (23) or if $p_0^{\sigma_{0,D}}(t) < p_1^{\sigma_{1,D}}(t) - L_1 - d$ holds for all $t' \geq t$; otherwise, $a_0(t) = a_{0,D}(t)$.

Intuitively, Queueing(d) and Following(d) represent typical policies based on the first and the second high-level decision in Section V-A, respectively.¹²

Now we set the motion of s_1 in simulations. Assume that s_1 starts from the position $p_1(0)$ and maintains the constant velocity 15 until it reaches the position $-(v_F^2 - 15^2)/(2a_F)$; then, it changes the acceleration to a_F until it reaches the position 0 with velocity v_F ; finally, it follows the constant velocity v_F until it releases the resource. Here, v_F is a free parameter; $a_F \triangleq a_{1,M}$ if $v_F \geq 15$ and $a_F \triangleq -a_{1,m}$ if $v_F < 15$. Furthermore, we assume that s_0 can always observe the real-time state of s_1 .

Fig. 10 provides the output trajectories of different policies for $p_1(0) = -160$ and $v_F = 15$. First, we can find that within the Queueing(d) policies and the Following(d) policies, the change of d provides different tradeoffs between $t_{0,\text{in}}$ and $v_0(t_{0,\text{in}})$, while the trend of the trajectories in each family is consistent. Second, the output trajectory of the proposed policy intuitively lies “between” the Queueing(d) policies and the Following(d) policies: the start time of deceleration is later than that of Following(d), which can preserve the possibility of occupying the resource before s_1 when the situation is still unclear; in contrast, it is earlier than that of Queueing(d), which can avoid a too small occupation velocity.

¹¹Here, $\sigma_{0,A}$, $\sigma_{0,D}$ and $\sigma_{1,D}$ represent the ACC or the DEC trajectory of s_0 or s_1 on $[t, +\infty)$, respectively.

¹²Precisely speaking, we use the step-wise version of Queueing(d) and Following(d) in simulations, while we will not discuss here in detail.

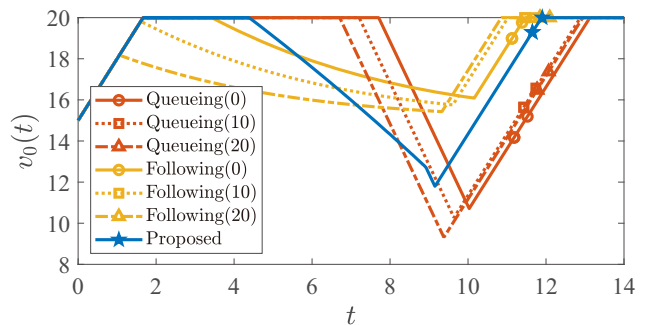


Fig. 10: The output trajectories of the proposed policy, Queueing(d) policies and Following(d) policies. Parameters $v_M = 20$, $a_{0,m} = a_{1,m} = 4$, $a_{0,M} = a_{1,M} = 3$, $L_0 = L_1 = 5$, $t_k = 0.01k$, $p_0(0) = -200$, $v_0(0) = 15$, $p_1(0) = -160$, and $v_F = 15$. On each curve, the two markers represent $t = t_{0,\text{in}}$ and $t = t_{0,\text{out}}$.

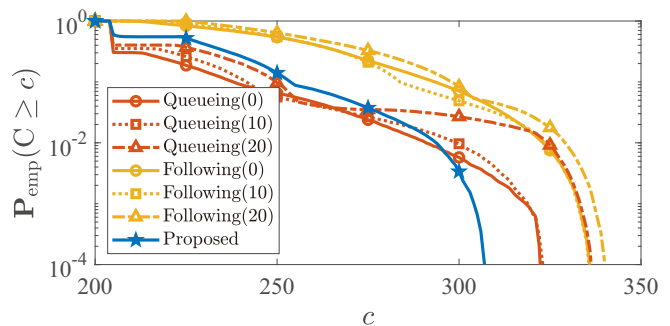


Fig. 11: The tail empirical probability $\mathbb{P}_{\text{emp}}(C \geq c)$ for the proposed policy, Queueing(d) policies and Following(d) policies. Parameters $v_M = 20$, $a_{0,m} = a_{1,m} = 4$, $a_{0,M} = a_{1,M} = 3$, $L_0 = L_1 = 5$, $t_k = 0.01(k - 1)$, $p_0(0) = -200$, and $v_0(0) = 15$. For each curve, 10^5 experiments are performed.

This observation coincides with our intuition in Section V-A. Furthermore, we can also find that the proposed policy turns from deceleration to acceleration *earliest* among all policies.

Now we perform 10^5 random experiments by choosing $p_1(0)$ uniformly in $[-200, -100]$ and choosing v_F uniformly in $[5, 20]$. The tail empirical probability of the scheduling cost C , i.e.,

$$\mathbb{P}_{\text{emp}}(C \geq c) \triangleq 10^{-5} \cdot \text{card}\{n \mid C^{(n)} \geq c\} \quad (54)$$

is shown in Fig. 11, where $C^{(n)}$ represents the scheduling cost in the n -th experiment. As shown in the figure, if we allow an outage probability of 10^{-4} , the largest cost of the proposed policy is 306.9, while the largest costs of the other six policies are higher than 322.4. By discarding the ineliminable constant 204.2 from both values,¹³ this is a reduction by 13.4%. Therefore, the simulation result verifies the robustness of the proposed policy against the trajectory uncertainty of s_1 .

C. Effect of Decision and Observation Periods

In this subsection, we evaluate the effect of different decision periods and observation periods on the output trajectory. Specifically, the motion of s_1 is the same as the last subsection

¹³This ineliminable constant part of the cost results from the initial state $\mathbf{x}_0(0) = \langle -200, 15 \rangle$ of s_0 .

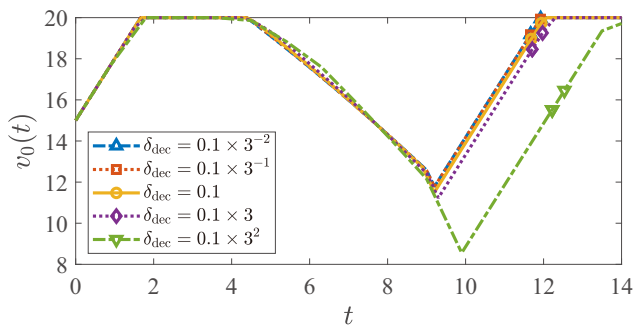


Fig. 12: The output trajectories of the proposed policy with different decision periods δ_{dec} . Parameters $v_M = 20$, $a_{0,m} = a_{1,m} = 4$, $a_{0,M} = a_{1,M} = 3$, $L_0 = L_1 = 5$, $p_0(0) = -200$, $v_0(0) = 15$, $p_1(0) = -160$, $v_F = 15$ and $\delta_{\text{obs}} = 0.1$. On each curve, the two markers represent $t = t_{0,\text{in}}$ and $t = t_{0,\text{out}}$.

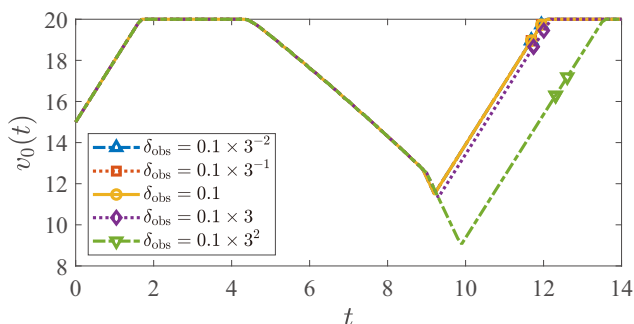


Fig. 13: The output trajectories of the proposed policy with different observation periods δ_{obs} . Parameters $v_M = 20$, $a_{0,m} = a_{1,m} = 4$, $a_{0,M} = a_{1,M} = 3$, $L_0 = L_1 = 5$, $p_0(0) = -200$, $v_0(0) = 15$, $p_1(0) = -160$, $v_F = 15$ and $\delta_{\text{dec}} = 0.1$. On each curve, the two markers represent $t = t_{0,\text{in}}$ and $t = t_{0,\text{out}}$. Note that the first three curves coincide.

with $p_1(0) = -160$ and $v_F = 15$, and we assume that s_0 can observe the real-time state of s_1 at times $m\delta_{\text{obs}}$ ($m \geq 0$). The decision times t_k are set to $k\delta_{\text{dec}}$.

Fig. 12 and Fig. 13 illustrate the output trajectories for different δ_{dec} and δ_{obs} , respectively. According to the two figures, the safety of the system can always be guaranteed, and we can also find that both δ_{dec} and δ_{obs} have little effect on the performance as long as they are small enough (smaller than 0.3 under the given parameters). Intuitively, “small enough” means that the velocity of s_1 should not change much during a period, i.e.,

$$\delta_{\text{dec}}, \delta_{\text{obs}} \ll \min \left\{ \frac{v_M}{a_{1,m}}, \frac{v_M}{a_{1,M}} \right\}. \quad (55)$$

After that, more frequent decisions or observations will no longer improve the performance.

D. Effect of Different Inertial Constraints

In this subsection, we discuss the effect of different inertial constraints of s_0 and s_1 , i.e., the bounds on their accelerations $\langle a_{0,m}, a_{0,M} \rangle$ and $\langle a_{1,m}, a_{1,M} \rangle$. For the motion of s_1 , we still use the one proposed in Section VI-B with $v_F = 15$. Then the relations between the scheduling cost C and $p_1(0)$ for different $\langle a_{0,m}, a_{0,M} \rangle$ and $\langle a_{1,m}, a_{1,M} \rangle$ are shown in Fig. 14 and Fig.

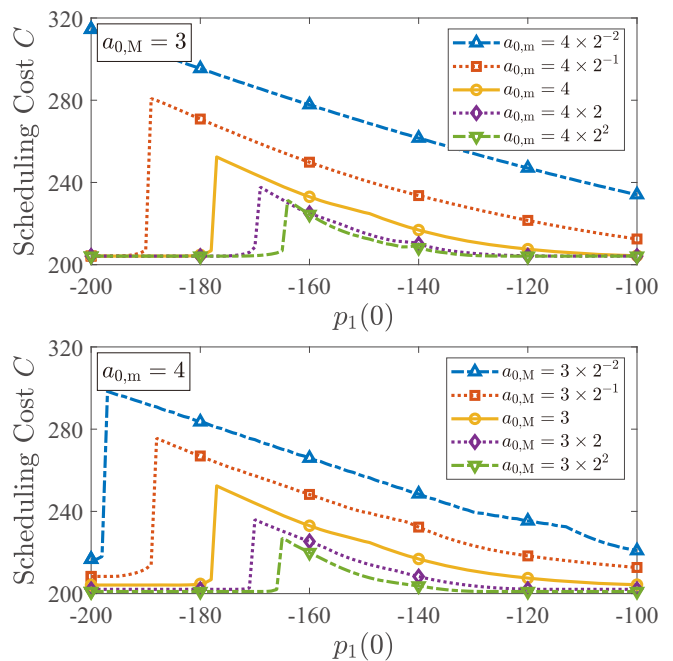


Fig. 14: The scheduling cost C of the proposed policy. Parameters $v_M = 20$, $a_{1,m} = 4$, $a_{1,M} = 3$, $L_0 = L_1 = 5$, $t_k = 0.01(k-1)$, $p_0(0) = -200$, $v_0(0) = 15$ and $v_F = 15$.

15, respectively. Note that all curves are discontinuous: the left (or right) side of the discontinuity means that s_0 occupies the resource before (or after) s_1 .

According to Fig. 14, the changes of $a_{0,m}$ and $a_{0,M}$ have similar effects on the scheduling cost, since both of them affect the *control ability* of s_0 . Clearly, larger $a_{0,m}$ and $a_{0,M}$ mean that s_0 can adjust the state more free, and thus it can delay the determination on whether to occupy the resource before or after s_1 until the situation becomes more clear, which can generally result in a smaller cost.

In contrast, $a_{1,m}$ and $a_{1,M}$ is related to the *information collection ability* of s_0 . As shown in Fig. 15, the effect of $a_{1,m}$ mainly occurs when s_0 occupies the resource after s_1 . Intuitively, a smaller $a_{1,m}$ means that s_0 can better estimate $t_{1,\text{out}}$ in advance, which earns more time for it to make preparations. On the other hand, the change of $a_{1,M}$ influences the position of the discontinuity point, since a smaller $a_{1,M}$ can eliminate possible conflicts caused by the acceleration of s_1 , which can enable s_0 to safely occupy the resource before s_1 in some critical cases.

VII. CONCLUSION

This article established a minimax scheduling framework for the system with two inertially constrained agents from the perspective of one agent, where the future trajectory of the other agent is unknown. A control policy was provided where a minimax optimization problem is solved at each decision time, in which the objective function is the state value function for a given situation; the inner maximum is over all possible situations, i.e., the uncertainty sets of the occupation time period of the other agent, for the next decision time; and the outer minimization is over all feasible target states at the next

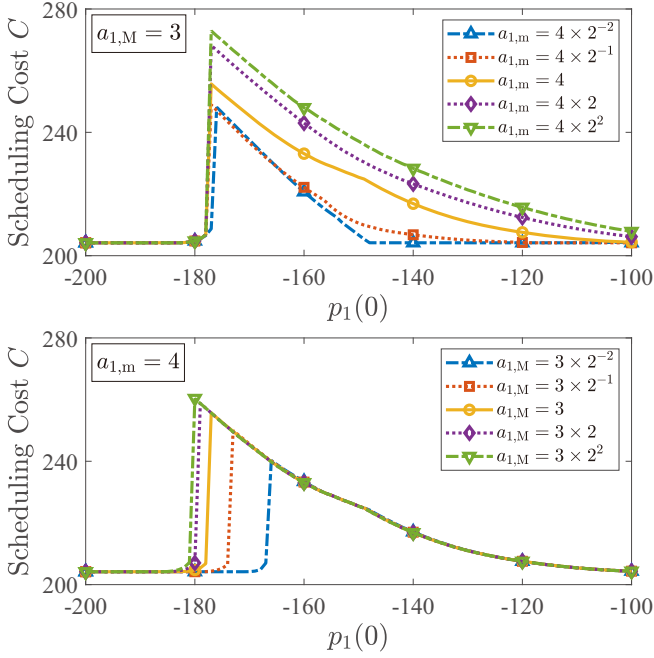


Fig. 15: The scheduling cost C of the proposed policy. Parameters $v_M = 20$, $a_{0,m} = 4$, $a_{0,M} = 3$, $L_0 = L_1 = 5$, $t_k = 0.01(k-1)$, $p_0(0) = -200$, $v_0(0) = 15$ and $v_F = 15$.

decision time. Calculation methods and the safety guarantee were also presented in the article. Furthermore, numerical simulations were performed comparing the proposed policy with queuing policies and following policies, showing the robustness of our policy against different motion modes of the other agent. In conclusion, the minimax framework provides an effective solution for the scheduling problem of two non-cooperative agents with inertial constraints.

APPENDIX

In Appendix A, we provide some lemmas to simplify further analyses. Then we present proofs in Appendices B-I for the theoretical results in the article.

A. Lemmas

The first lemma is a general property in kinematics, which can be directly verified by definition.

Lemma 1: Let $t_1, t_2 \in \mathbb{R}_+$ with $t_1 < t_2$. Consider two trajectories σ_1, σ_2 of s_i .

- (i) If $p_i^{\sigma_1}(t_1) = p_i^{\sigma_2}(t_1)$, and $v_i^{\sigma_1}(t) \geq v_i^{\sigma_2}(t)$ for all $t \in [t_1, t_2]$, then

$$p_i^{\sigma_1}(t_2) \geq p_i^{\sigma_2}(t_2). \quad (56)$$

- (ii) If $p_i^{\sigma_1}(t_1) = p_i^{\sigma_2}(t_1) \leq 0$, and $v_i^{\sigma_1}(t) \geq v_i^{\sigma_2}(t)$ for all $t \in [t_1, +\infty)$, then

$$t_{i,\text{in}}^{\sigma_1} \leq t_{i,\text{in}}^{\sigma_2}. \quad (57)$$

- (iii) If $p_i^{\sigma_1}(t_1) = p_i^{\sigma_2}(t_1) \leq L_i$, and $v_i^{\sigma_1}(t) \geq v_i^{\sigma_2}(t)$ for all $t \in [t_1, +\infty)$, then

$$t_{i,\text{out}}^{\sigma_1} \leq t_{i,\text{out}}^{\sigma_2}. \quad (58)$$

The next lemma characterizes the property of the DEC-ACC trajectories. Similar results for ACC-DEC trajectories also exist by exchanging “non-decreasing” and “non-increasing”, and we leave out detailed expressions.

Lemma 2: Let σ be a DEC-ACC trajectory of s_i on some interval $[t_0, +\infty)$ with a fixed state at t_0 . Then

- (i) For any fixed $t \geq t_0$, $p_i^\sigma(t)$ and $v_i^\sigma(t)$ are continuous and non-increasing with respect to t_D^σ ;
- (ii) $t_{i,\text{in}}^\sigma$ and $t_{i,\text{out}}^\sigma$ are continuous and non-decreasing with respect to t_D^σ ;
- (iii) $v_i^\sigma(t_{i,\text{in}}^\sigma)$ is non-increasing with respect to t_D^σ .

Proof: (i) Note that the closed-form expression of $p_i^\sigma(t)$ and $v_i^\sigma(t)$ can be calculated according to Definition 3, and the result can be directly checked.

(ii) The monotonicity can be obtained by part (i) and the definitions (5) and (6). The continuity can be verified by separately considering the case $p_i^\sigma(t_0) + \frac{v_i^\sigma(t_0)^2}{2a_m} > 0$ (or $> L$) and the case $p_i^\sigma(t_0) + \frac{v_i^\sigma(t_0)^2}{2a_m} \leq 0$ (or $\leq L$), which is also straightforward.

(iii) Let σ_1 and σ_2 be two DEC-ACC trajectories with $t_D^{\sigma_1} < t_D^{\sigma_2}$, and thus we have

$$v_i^{\sigma_1}(t_D^{\sigma_1}) \geq v_i^{\sigma_2}(t_D^{\sigma_2}). \quad (59)$$

Now we prove by contradiction. Assume that

$$v_i^{\sigma_1}(t_{i,\text{in}}^{\sigma_1}) < v_i^{\sigma_2}(t_{i,\text{in}}^{\sigma_2}) \quad (60)$$

then we must have

$$t_{i,\text{in}}^{\sigma_2} - t_D^{\sigma_2} > t_{i,\text{in}}^{\sigma_1} - t_D^{\sigma_1} \triangleq \Delta \quad (61)$$

which yields

$$v_i^{\sigma_1}(t_{i,\text{in}}^{\sigma_1} - \delta) < v_i^{\sigma_2}(t_{i,\text{in}}^{\sigma_2} - \delta), \quad \forall \delta \in [0, \Delta]. \quad (62)$$

Therefore,

$$\begin{aligned} 0 &= p_i^{\sigma_1}(t_{i,\text{in}}^{\sigma_1}) \\ &= (p_i^{\sigma_1}(t_{i,\text{in}}^{\sigma_1}) - p_i^{\sigma_1}(t_D^{\sigma_1})) + p_i^{\sigma_1}(t_D^{\sigma_1}) \\ &< (p_i^{\sigma_2}(t_{i,\text{in}}^{\sigma_2}) - p_i^{\sigma_2}(t_{i,\text{in}}^{\sigma_2} - \Delta)) + p_i^{\sigma_2}(t_D^{\sigma_1}) \\ &\leq p_i^{\sigma_2}(t_{i,\text{in}}^{\sigma_2}) = 0 \end{aligned} \quad (63)$$

which is a contradiction. \square

The next lemma claims that among all trajectories with the same $t_{i,\text{in}}$, the DEC-ACC trajectory serves as the upper bound for $v_i(t_{i,\text{in}})$. Similarly, the ACC-DEC trajectory serves as the lower bound, and we leave out detailed expressions.

Lemma 3: Let σ be a DEC-ACC trajectory of s_i on some interval $[t_0, +\infty)$. Then for any trajectory σ' with the same initial state at t_0 and satisfying $t_{i,\text{in}}^{\sigma'} = t_{i,\text{in}}^{\sigma} \triangleq t_{\text{in}}$, we have

$$v_i^{\sigma'}(t_{\text{in}}) \leq v_i^\sigma(t_{\text{in}}). \quad (64)$$

Proof: By the continuity in Lemma 2(i), there exists another DEC-ACC trajectory σ_1 such that

$$v_i^{\sigma_1}(t_{\text{in}}) = v_i^{\sigma'}(t_{\text{in}}). \quad (65)$$

Note that by the definition of the DEC-ACC trajectory, for any $t \in [t_{\text{cur}}, t_{\text{in}}]$, we have

$$\begin{aligned} v_i^{\sigma'}(t) &\geq \max \{v_i^{\sigma'}(t_{\text{cur}}) - a_m(t - t_{\text{cur}}), \\ &\quad v_i^{\sigma'}(t_{\text{in}}) - a_m(t_{\text{in}} - t), 0\} \\ &= v_i^{\sigma_1}(t). \end{aligned} \quad (66)$$

According to Lemma 1, we have

$$p_i^{\sigma_1}(t_{\text{in}}) \leq p_i^{\sigma'}(t_{\text{in}}) = 0 = p_i^{\sigma}(t_{\text{in}}) \quad (67)$$

and then by Lemma 2(i), we have $t_D^{\sigma_1} \geq t_D^{\sigma}$ and

$$v_i^{\sigma_1}(t_{\text{in}}) \leq v_i^{\sigma}(t_{\text{in}}). \quad (68)$$

By (65) and (68), the proof is completed. \square

B. Proof of Proposition 1 in Section III-A

Proof: (i) For any trajectory σ of s_1 , $t_{1,\text{in}}^{\sigma_A} \leq t_{1,\text{in}}^{\sigma} \leq t_{1,\text{in}}^{\sigma_D}$ holds by Lemma 1(ii). According to Lemma 3, we have

$$v_1^{\sigma_{\text{AD}}(t_{1,\text{in}}^{\sigma})}(t_{1,\text{in}}^{\sigma}) \leq v_1^{\sigma}(t_{1,\text{in}}^{\sigma}) \leq v_1^{\sigma_{\text{DA}}(t_{1,\text{in}}^{\sigma})}(t_{1,\text{in}}^{\sigma}). \quad (69)$$

Then by Lemma 1(iii),

$$t_{1,\text{out}}^{\sigma_{\text{DA}}(t_{1,\text{in}}^{\sigma})} \leq t_{1,\text{out}}^{\sigma} \leq t_{1,\text{out}}^{\sigma_{\text{AD}}(t_{1,\text{in}}^{\sigma})}. \quad (70)$$

Therefore, $\langle \hat{t}_{1,\text{in}}^{\sigma}, \hat{t}_{1,\text{out}}^{\sigma} \rangle \in \mathcal{I}$.

(ii) For any trajectory σ of s_1 , $t_{1,\text{out}}^{\sigma_A} \leq t_{1,\text{out}}^{\sigma} \leq t_{1,\text{out}}^{\sigma_D}$ holds by Lemma 1(iii). Therefore, $\langle \hat{t}_{1,\text{in}}^{\sigma}, \hat{t}_{1,\text{out}}^{\sigma} \rangle \in \mathcal{I}$.

(iii) The result is obvious. \square

C. Proof of Proposition 2 in Section III-A

Proof: The claims in the first sentence are clear. For the monotonicity, we only need to consider the case (i) in Proposition 1. A further observation is that we only need to show that $t_{1,\text{out}}^{\sigma_{\text{DA}}(t_{1,\text{in}})} - t_{1,\text{in}}$ and $t_{1,\text{out}}^{\sigma_{\text{AD}}(t_{1,\text{in}})} - t_{1,\text{in}}$ are non-decreasing with respect to $t_{1,\text{in}}$.

Let $t_{1,\text{in}}^{(1)} \leq t_{1,\text{in}}^{(2)}$. By Lemma 2(ii), we have

$$t_D^{\sigma_{\text{DA}}(t_{1,\text{in}}^{(1)})} \leq t_D^{\sigma_{\text{DA}}(t_{1,\text{in}}^{(2)})} \quad (71)$$

and by Lemma 2(iii),

$$v_1^{\sigma_{\text{DA}}(t_{1,\text{in}}^{(1)})}(t_{1,\text{in}}^{(1)}) \geq v_1^{\sigma_{\text{DA}}(t_{1,\text{in}}^{(2)})}(t_{1,\text{in}}^{(2)}) \quad (72)$$

Then according to Lemma 1(iii), we have

$$t_{1,\text{out}}^{\sigma_{\text{DA}}(t_{1,\text{in}}^{(1)})} - t_{1,\text{in}}^{(1)} \leq t_{1,\text{out}}^{\sigma_{\text{DA}}(t_{1,\text{in}}^{(2)})} - t_{1,\text{in}}^{(2)}. \quad (73)$$

Similarly, the monotonicity of $t_{1,\text{out}}^{\sigma_{\text{AD}}(t_{1,\text{in}})} - t_{1,\text{in}}$ can also be obtained. \square

D. Proof of Proposition 3 in Section III-B

Proof: The proof of (27) is divided into two steps. First, we show that for any trajectory of s_0 in $\Sigma_0(\mathbf{x}; t_{\text{cur}})$ with finite manageable cost, we can find a DEC-ACC trajectory with an equal or smaller manageable cost. Then, we show that within the DEC-ACC trajectories, the trajectory σ^* has the smallest manageable cost.

For the first step, let $\sigma_0 \in \Sigma_0(\mathbf{x}; t_{\text{cur}})$ be a general trajectory with finite $C^*(\sigma_0; \mathcal{I})$. Then by the continuity in Lemma 2(ii), there exists a DEC-ACC trajectory σ such that $t_{0,\text{in}}^{\sigma} = t_{0,\text{in}}^{\sigma_0}$. Then by Lemma 3, we have

$$v_0^{\sigma}(t_{0,\text{in}}^{\sigma}) \geq v_0^{\sigma_0}(t_{0,\text{in}}^{\sigma_0}). \quad (74)$$

Therefore, $C^*(\sigma; \mathcal{I}) \leq C^*(\sigma_0; \mathcal{I})$, and σ is the trajectory we want for the first step.

The second step is the direct corollary of Lemma 2(ii) and (iii) that for a DEC-ACC trajectory σ , $t_{0,\text{in}}^{\sigma}$ is non-decreasing with t_D^{σ} and $v_0^{\sigma}(t_{0,\text{in}}^{\sigma})$ is non-increasing with t_D^{σ} . Thus (27) is proved.

Note that the last result in Proposition 3 is also included in the discussions above. Therefore, the proof is completed. \square

E. Proof of Theorem 1 in Section IV-A

Proof: We denote the final trajectory of s_0 by σ_* , and assume that $t_K < t_{0,\text{in}}^{\sigma_*} \leq t_{K+1}$. We also assume that the set of target states at t_k is $\mathcal{F}_{k,*}$, the information obtained at t_k is $\mathcal{I}_{k,*}$, and the range of \mathcal{I}_{k+1} based on $\mathcal{I}_{k,*}$ is $\mathcal{J}_{k,*}$. For $0 \leq k \leq K-1$, we define the following statement:

$$\mathcal{P}_k : \exists \mathbf{x}_{\text{tar}} \in \mathcal{F}_{k,*}, V_{\max}(\mathbf{x}_{\text{tar}}; t_{k+1}, \mathcal{I}_{k,*}) < +\infty. \quad (75)$$

by the definitions (37) and (26), \mathcal{P}_k is equivalent to

$$\begin{aligned} \mathcal{P}'_k : \exists \mathbf{x}_{\text{tar}} \in \mathcal{F}_{k,*}, \forall \mathcal{I}_{k+1} \in \mathcal{J}_{k,*}, \\ \exists \sigma \in \Sigma_0(\mathbf{x}_{\text{tar}}; t_{k+1}), C^*(\sigma; t_{k+1}, \mathcal{I}_{k+1}) < +\infty. \end{aligned} \quad (76)$$

By exchanging the order, the next statement is a sufficient condition for \mathcal{P}'_k :

$$\begin{aligned} \mathcal{Q}_k : \exists \mathbf{x}_{\text{tar}} \in \mathcal{F}_{k,*}, \exists \sigma \in \Sigma_0(\mathbf{x}_{\text{tar}}; t_{k+1}), \\ \forall \mathcal{I}_{k+1} \in \mathcal{J}_{k,*}, C^*(\sigma; t_{k+1}, \mathcal{I}_{k+1}) < +\infty. \end{aligned} \quad (77)$$

Then according to (24) and (26), we can successively check that \mathcal{Q}_k is equivalent to the three statements below:

$$\begin{aligned} \mathcal{Q}'_k : \exists \mathbf{x}_{\text{tar}} \in \mathcal{F}_{k,*}, \exists \sigma \in \Sigma_0(\mathbf{x}_{\text{tar}}; t_{k+1}), \\ C^*(\sigma; t_{k+1}, \max\{t_{k+1}, \mathcal{I}_{k,*}\}) < +\infty. \end{aligned} \quad (78)$$

$$\mathcal{Q}''_k : \exists \sigma \in \Sigma_0(\mathbf{x}_0^{\sigma_*}(t_k); t_k), C^*(\sigma; t_k, \mathcal{I}_{k,*}) < +\infty. \quad (79)$$

$$\mathcal{Q}'''_k : V(\mathbf{x}_0^{\sigma_*}(t_k); t_k, \mathcal{I}_{k,*}) < +\infty. \quad (80)$$

The definition of \mathcal{Q}''_k and \mathcal{Q}'''_k can also be extended to $k = K$.

Note that \mathcal{Q}''_0 is true by (8), and we have the logic chain

$$\mathcal{Q}''_k \Rightarrow \mathcal{P}_k \Rightarrow \mathcal{Q}'''_{k+1} \Leftrightarrow \mathcal{Q}''_{k+1} \quad (81)$$

for $k \leq K-1$, where the second inference comes from the choice of \mathbf{x}_{tar} in Algorithm 1. Then by induction, \mathcal{Q}''_K is true. Furthermore, note that when \mathcal{Q}''_K is true, Algorithm 1 can always return a trajectory satisfying the robust safety condition at time t_K , which is stronger than the safety condition (7). Thus we complete the proof. \square

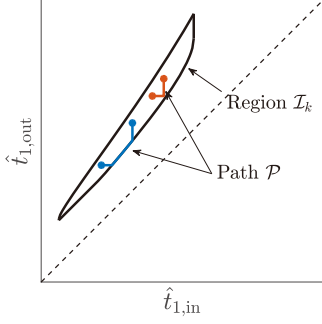


Fig. 16: Illustration of the constructions of the path \mathcal{P} in the proof of Proposition 6 for two pairs of points, which correspond to (84) (blue) and (85) (red), respectively.

F. Proof of Proposition 6 in Section IV-C

Proof: First, for a given $\mathcal{I}_{k+1} \subseteq \mathcal{I}_k$, there exist two points $\langle \hat{t}_{1,\text{in}}, t_* \rangle$ and $\langle t_{**}, \hat{t}_{1,\text{out}} \rangle$ in \mathcal{I}_{k+1} by (40) and (41). In addition, by the minimality of $\hat{t}_{1,\text{in}}$ and the maximality of $\hat{t}_{1,\text{out}}$, we have

$$\hat{t}_{1,\text{in}} \leq t_{**}, \quad \hat{t}_{1,\text{out}} \geq t_*. \quad (82)$$

Therefore, $\langle \hat{t}_{1,\text{in}}, \hat{t}_{1,\text{out}} \rangle \in \mathcal{B}(\mathcal{I}_k)$.

Conversely, let $\langle \hat{t}_{1,\text{in}}^{(1)}, \hat{t}_{1,\text{out}}^{(1)} \rangle, \langle \hat{t}_{1,\text{in}}^{(2)}, \hat{t}_{1,\text{out}}^{(2)} \rangle \in \mathcal{I}_k$, and we show that there exists $\mathcal{I}_{k+1} \subseteq \mathcal{I}_k$ satisfying Assumption 2 such that

$$\langle \hat{t}_{1,\text{in}}, \hat{t}_{1,\text{out}} \rangle = \langle \min\{\hat{t}_{1,\text{in}}^{(1)}, \hat{t}_{1,\text{in}}^{(2)}\}, \max\{\hat{t}_{1,\text{out}}^{(1)}, \hat{t}_{1,\text{out}}^{(2)}\} \rangle. \quad (83)$$

Now we separately consider the following two cases.

- If the right-hand side of (83) equals either $\langle \hat{t}_{1,\text{in}}^{(1)}, \hat{t}_{1,\text{out}}^{(1)} \rangle$ or $\langle \hat{t}_{1,\text{in}}^{(2)}, \hat{t}_{1,\text{out}}^{(2)} \rangle$, then \mathcal{I}_{k+1} can be chosen as the corresponding single-point set, which clearly satisfies Assumption 2.
- Otherwise, we assume that the right-hand side of (83) is equal to $\langle \hat{t}_{1,\text{in}}^{(1)}, \hat{t}_{1,\text{out}}^{(2)} \rangle$ without loss of generality. Consider a path \mathcal{P} connecting $\langle \hat{t}_{1,\text{in}}^{(1)}, \hat{t}_{1,\text{out}}^{(1)} \rangle$ and $\langle \hat{t}_{1,\text{in}}^{(2)}, \hat{t}_{1,\text{out}}^{(2)} \rangle$, which is defined as follows: if $\hat{t}_{1,\text{in}}(\hat{t}_{1,\text{out}}^{(1)}) \leq \hat{t}_{1,\text{in}}^{(2)}$, then

$$\begin{aligned} \mathcal{P} \triangleq & \left\{ \langle t_*, \hat{t}_{1,\text{out}}^{(1)} \rangle \mid \hat{t}_{1,\text{in}}^{(1)} \leq t_* \leq \hat{t}_{1,\text{in}}(\hat{t}_{1,\text{out}}^{(1)}) \right\} \\ & \cup \left\{ \langle t_*, \hat{t}_{1,\text{out}}(t_*) \rangle \mid \hat{t}_{1,\text{in}}(\hat{t}_{1,\text{out}}^{(1)}) \leq t_* \leq \hat{t}_{1,\text{in}}^{(2)} \right\} \\ & \cup \left\{ \langle \hat{t}_{1,\text{in}}^{(2)}, t_* \rangle \mid \hat{t}_{1,\text{out}}(\hat{t}_{1,\text{in}}^{(2)}) \leq t_* \leq \hat{t}_{1,\text{out}}^{(2)} \right\} \end{aligned} \quad (84)$$

and otherwise

$$\begin{aligned} \mathcal{P} \triangleq & \left\{ \langle t_*, \hat{t}_{1,\text{out}}^{(1)} \rangle \mid \hat{t}_{1,\text{in}}^{(1)} \leq t_* \leq \hat{t}_{1,\text{in}}^{(2)} \right\} \\ & \cup \left\{ \langle \hat{t}_{1,\text{in}}^{(2)}, t_* \rangle \mid \hat{t}_{1,\text{out}}^{(1)} \leq t_* \leq \hat{t}_{1,\text{out}}^{(2)} \right\} \end{aligned} \quad (85)$$

where

$$\hat{t}_{1,\text{in}}(\cdot) \triangleq \max\{t_* \mid \langle t_*, \cdot \rangle \in \mathcal{I}_k\} \quad (86)$$

$$\hat{t}_{1,\text{out}}(\cdot) \triangleq \min\{t_* \mid \langle \cdot, t_* \rangle \in \mathcal{I}_k\}. \quad (87)$$

The construction of the path \mathcal{P} is shown in Fig. 16. By using Assumption 2 on \mathcal{I}_k , we can show that \mathcal{P} also satisfies Assumption 2. Therefore, by choosing $\mathcal{I}_{k+1} = \mathcal{P}$, (83) holds.

Thus we complete the proof. \square

G. Proof of Proposition 7 in Section IV-C

Proof: For (44), assume $\bar{t}^{(1)} \geq \bar{t}^{(2)}$ without loss of generality. Then we only need to show $\langle \underline{t}^{(2)}, \bar{t}^{(1)} \rangle \in \mathcal{B}(\mathcal{I}_k)$.

Since $\langle \underline{t}^{(1)}, \bar{t}^{(1)} \rangle, \langle \underline{t}^{(2)}, \bar{t}^{(2)} \rangle \in \mathcal{B}(\mathcal{I}_k)$, there must exist $t_* \geq \underline{t}^{(1)}$ and $t_{**} \leq \bar{t}^{(2)}$ such that $\langle t_*, \bar{t}^{(1)} \rangle, \langle \underline{t}^{(2)}, t_{**} \rangle \in \mathcal{I}_k$. Clearly, we have

$$t_{**} \leq \bar{t}^{(2)} \leq \bar{t}^{(1)}. \quad (88)$$

Now we choose

$$t_* = \max\{t \mid \langle t, \bar{t}^{(1)} \rangle \in \mathcal{I}_k\} \quad (89)$$

and we aim to show $t_* \geq \underline{t}^{(2)}$ by contradiction. First, let $\hat{t}_{1,\text{out}}(\cdot)$ and $\hat{t}_{1,\text{in}}(\cdot)$ be defined by

$$\hat{t}_{1,\text{out}}(t), \hat{t}_{1,\text{in}}(t) \triangleq \mathcal{I}_k \cap \{t_{1,\text{in}} = t\} \quad (90)$$

if it is non-empty. By $\langle t_*, \bar{t}^{(1)} \rangle, \langle \underline{t}^{(2)}, t_{**} \rangle \in \mathcal{I}_k$, both $\hat{t}_{1,\text{out}}(\cdot)$ and $\hat{t}_{1,\text{in}}(\cdot)$ are well-defined at t_* and $\underline{t}^{(2)}$. Suppose $t_* < \underline{t}^{(2)}$, and then by Assumption 2, we have

$$\bar{t}^{(1)} \leq \hat{t}_{1,\text{out}}(t_*) \leq \hat{t}_{1,\text{out}}(\underline{t}^{(2)}). \quad (91)$$

Since we also have $\hat{t}_{1,\text{out}}(\underline{t}^{(2)}) \leq \bar{t}^{(2)} \leq \bar{t}^{(1)}$, it can be concluded that $\langle \underline{t}^{(2)}, \bar{t}^{(1)} \rangle \in \mathcal{I}_k$, which contradicts with (89). Hence, $t_* \geq \underline{t}^{(2)}$.

Finally, by $\langle t_*, \bar{t}^{(1)} \rangle, \langle \underline{t}^{(2)}, t_{**} \rangle \in \mathcal{I}_k$, $t_{**} \leq \bar{t}^{(1)}$ and $t_* \geq \underline{t}^{(2)}$, we have $\langle \underline{t}^{(2)}, \bar{t}^{(1)} \rangle \in \mathcal{B}(\mathcal{I}_k)$ according to Proposition 6.

Another result (45) can be similarly proved. \square

H. Proof of Theorem 2 in Section IV-C

Proof: (i) On \mathcal{D}_1 , we have $t_{0,\text{out}}^{\sigma_A} \leq \bar{t}$. Recall that the interval (\underline{t}, \bar{t}) corresponds to $\mathcal{W}(\mathcal{I}_{k+1})$ according to (39). Therefore, σ_A satisfies the robust safety condition $(t_{0,\text{in}}^{\sigma_A}, t_{0,\text{out}}^{\sigma_A}) \cap \mathcal{W}(\mathcal{I}_{k+1}) = \emptyset$. Since σ_A is the DEC-ACC trajectory with the smallest t_D , by Proposition 3, we have

$$\begin{aligned} V(\underline{t}, \bar{t}) &= C^*(\sigma_A; t_{k+1}, \mathcal{I}_{k+1}) \\ &= v_M(t_{0,\text{in}}^{\sigma_A} - t_{k+1}) + \frac{(v_M - v_0^{\sigma_A}(t_{0,\text{in}}^{\sigma_A}))^2}{2a_{0,M}} \end{aligned} \quad (92)$$

which is a constant with respect to $\langle \underline{t}, \bar{t} \rangle$.

(ii) Similar to (i), σ_A also satisfies the robust safety condition on \mathcal{D}_2 , and we have

$$\begin{aligned} V(\underline{t}, \bar{t}) &= C^*(\sigma_A; t_{k+1}, \mathcal{I}_{k+1}) \\ &= v_M[(t_{0,\text{in}}^{\sigma_A} - t_{k+1}) - (\bar{t} - \underline{t})] + \frac{(v_M - v_0^{\sigma_A}(t_{0,\text{in}}^{\sigma_A}))^2}{2a_{0,M}}. \end{aligned} \quad (93)$$

Then the results can be simply checked.

(iii) On \mathcal{D}_3 , σ_A does not satisfy the robust safety condition. By Proposition 3, the best trajectory is $\sigma_{\text{DA}}(\bar{t})$ if it exists, i.e., the DEC-ACC trajectory satisfying $t_{0,\text{in}} = \bar{t}$. Hence,

$$V(\underline{t}, \bar{t}) = v_M(\underline{t} - t_{k+1}) + \frac{(v_M - v_0^{\sigma_{\text{DA}}(\bar{t})}(\bar{t}))^2}{2a_{0,M}} \quad (94)$$

which is clearly non-decreasing with \underline{t} , and is also non-decreasing with \bar{t} according to Lemma 2(iii) in Appendix A.

Furthermore, note that $\sigma_{DA}(\bar{t})$ does not exist if and only if $\bar{t} > t_{0,in}^{\sigma_D}$, where σ_D is the DEC trajectory of s_0 on $[t_{k+1}, +\infty)$, and in this case we have $V(\underline{t}, \bar{t}) = +\infty$. Therefore, the monotonicity results remain true. \square

I. Proof of Proposition 8 in Section IV-C

Proof: (i) The result is direct by Theorem 2(i).

(ii) First, it is easy to show that (50) lies in $\mathcal{B}(\mathcal{I}_k) \cap \mathcal{D}_2$ by Assumption 2 and (48). According to Theorem 2(ii), the optimal point in $\mathcal{B}(\mathcal{I}_k) \cap \mathcal{D}_2$ is obtained at the point with minimum $\bar{t} - \underline{t}$. Assume that this minimum occurs at some point $(\underline{t}_*, \bar{t}_*)$, and we must have $\bar{t}_* = \hat{t}_{1,out}(\underline{t}_*)$ due to the minimality. Then by Assumption 2, \underline{t}_* should also be chosen as the smallest value, which results in the point (50).

(iii) According to Theorem 2(iii), we only need to show the point (51) lies in $\mathcal{B}(\mathcal{I}_k) \cap \mathcal{D}_3$. This is also straightforward by Proposition 7 and (49). \square

REFERENCES

- [1] J. Wan, S. Tang, Z. Shu *et al.*, "Software-defined industrial internet of things in the context of industry 4.0," *IEEE Sensors J.*, vol. 16, no. 20, pp. 7373–7380, Oct. 2016.
- [2] E. Sisinni, A. Saifullah, S. Han *et al.*, "Industrial internet of things: Challenges, opportunities, and directions," *IEEE Trans. Ind. Informat.*, vol. 14, no. 11, pp. 4724–4734, Nov. 2018.
- [3] R. Olfati-Saber, "Flocking for multi-agent dynamic systems: algorithms and theory," *IEEE Trans. Autom. Control*, vol. 51, no. 3, pp. 401–420, Mar. 2006.
- [4] G. Karagiannis, O. Altintas, E. Ekici *et al.*, "Vehicular networking: A survey and tutorial on requirements, architectures, challenges, standards and solutions," *IEEE Commun. Surveys Tuts.*, vol. 13, no. 4, pp. 584–616, Fourth Quarter 2011.
- [5] J. Levinson, J. Askeland, J. Becker *et al.*, "Towards fully autonomous driving: Systems and algorithms," in *Proc. IEEE Intell. Veh. Symp.*, vol. 1, Baden-Baden, Germany, Jul. 2011, pp. 163–168.
- [6] L. Gupta, R. Jain, and G. Vaszkun, "Survey of important issues in UAV communication networks," *IEEE Commun. Surveys Tuts.*, vol. 18, no. 2, pp. 1123–1152, Second Quarter 2016.
- [7] R. Olfati-Saber, J. A. Fax, and R. M. Murray, "Consensus and cooperation in networked multi-agent systems," *Proc. IEEE*, vol. 95, no. 1, pp. 215–233, Jan. 2007.
- [8] J. R. Marden, G. Arslan, and J. S. Shamma, "Cooperative control and potential games," *IEEE Trans. Syst., Man, Cybern. B*, vol. 39, no. 6, pp. 1393–1407, Dec. 2009.
- [9] Y. Cao, W. Yu, W. Ren *et al.*, "An overview of recent progress in the study of distributed multi-agent coordination," *IEEE Trans. Ind. Informat.*, vol. 9, no. 1, pp. 427–438, Feb. 2013.
- [10] Y. Cai and Y. Shen, "An integrated localization and control framework for multi-agent formation," *IEEE Trans. Signal Process.*, vol. 67, no. 7, pp. 1941–1956, Apr. 2019.
- [11] R. W. Conway, W. L. Maxwell, and L. W. Miller, *Theory of scheduling*. Boston, USA: Addison-Wesley Publishing Company, 1967.
- [12] R. Graham, E. Lawler, J. Lenstra *et al.*, "Optimization and approximation in deterministic sequencing and scheduling: a survey," *Ann. Discrete Math.*, vol. 5, pp. 287–326, 1979.
- [13] P. Brucker, A. Drexler, R. Möhring *et al.*, "Resource-constrained project scheduling: Notation, classification, models, and methods," *Europ. J. Oper. Res.*, vol. 112, no. 1, pp. 3–41, Jan. 1999.
- [14] D. Merkle, M. Middendorf, and H. Schmeck, "Ant colony optimization for resource-constrained project scheduling," *IEEE Trans. Evol. Comput.*, vol. 6, no. 4, pp. 333–346, Nov. 2002.
- [15] L. Tassiulas and A. Ephremides, "Stability properties of constrained queueing systems and scheduling policies for maximum throughput in multihop radio networks," *IEEE Trans. Autom. Control*, vol. 37, no. 12, pp. 1936–1948, Dec. 1992.
- [16] Q. Wu, Y. Zeng, and R. Zhang, "Joint trajectory and communication design for multi-UAV enabled wireless networks," *IEEE Trans. Wireless Commun.*, vol. 17, no. 3, pp. 2109–2121, Jan. 2018.
- [17] I. Kadota, A. Sinha, E. Uysal-Biyikoglu *et al.*, "Scheduling policies for minimizing age of information in broadcast wireless networks," *IEEE/ACM Trans. Netw.*, vol. 26, no. 6, pp. 2637–2650, Oct. 2018.
- [18] S. E. Mahmoodi, R. N. Uma, and K. P. Subbalakshmi, "Optimal joint scheduling and cloud offloading for mobile applications," *IEEE Trans. on Cloud Comput.*, vol. 7, no. 2, Apr. 2019.
- [19] L. Chen and C. Englund, "Cooperative intersection management: A survey," *IEEE Trans. Intell. Transp. Syst.*, vol. 17, no. 2, pp. 570–586, Feb. 2016.
- [20] J. Rios-Torres and A. A. Malikopoulos, "A survey on the coordination of connected and automated vehicles at intersections and merging at highway on-ramps," *IEEE Trans. Intell. Transp. Syst.*, vol. 18, no. 5, pp. 1066–1077, May 2017.
- [21] D. Zhao, Y. Dai, and Z. Zhang, "Computational intelligence in urban traffic signal control: A survey," *IEEE Trans. Syst., Man, Cybern. C*, vol. 42, no. 4, pp. 485–494, Jul. 2012.
- [22] J. Gregoire, X. Qian, E. Frazzoli *et al.*, "Capacity-aware backpressure traffic signal control," *IEEE Trans. Control Netw. Syst.*, vol. 2, no. 2, pp. 164–173, Jun. 2015.
- [23] H. Yang, H. Rakha, and M. V. Ala, "Eco-cooperative adaptive cruise control at signalized intersections considering queue effects," *IEEE Trans. Intell. Transp. Syst.*, vol. 18, no. 6, pp. 1575–1585, Jun. 2017.
- [24] B. Xu, X. J. Ban, Y. Bian *et al.*, "Cooperative method of traffic signal optimization and speed control of connected vehicles at isolated intersections," *IEEE Trans. Intell. Transp. Syst.*, vol. 20, no. 4, pp. 1390–1403, Apr. 2019.
- [25] T. T. Phan, D. Ngoduy, and L. B. Le, "Space distribution method for autonomous vehicles at a signalized multi-lane intersection," *IEEE Trans. Intell. Transp. Syst.*, vol. 21, no. 12, pp. 5283–5294, Dec. 2020.
- [26] H. Kowshik, D. Caveney, and P. R. Kumar, "Provable systemwide safety in intelligent intersections," *IEEE Trans. Veh. Technol.*, vol. 60, no. 3, pp. 804–818, Mar. 2011.
- [27] S. Huang, A. W. Sadek, and Y. Zhao, "Assessing the mobility and environmental benefits of reservation-based intelligent intersections using an integrated simulator," *IEEE Trans. Intell. Transp. Syst.*, vol. 13, no. 3, pp. 1201–1214, Sep. 2012.
- [28] K. Zhang, D. Zhang, A. de La Fortelle *et al.*, "State-driven priority scheduling mechanisms for driverless vehicles approaching intersections," *IEEE Trans. Intell. Transp. Syst.*, vol. 16, no. 5, pp. 2487–2500, Oct. 2015.
- [29] F. Yang and Y. Shen, "An adaptive approach for intersection vehicle scheduling with limited state information," in *Proc. IEEE Int. Conf. Intell. Transp. Syst.*, vol. 1, Rhodes, Greece, Sep. 2020, pp. 1–6.
- [30] J. Wu, F. Perronnet, and A. Abbas-Turki, "Cooperative vehicle-actuator system: a sequence-based framework of cooperative intersections management," *IET Intell. Transp. Syst.*, vol. 8, no. 4, pp. 352–360, Jun. 2014.
- [31] P. Lin, J. Liu, P. J. Jin *et al.*, "Autonomous vehicle-intersection coordination method in a connected vehicle environment," *IEEE Intell. Transp. Syst. Mag.*, vol. 9, no. 4, pp. 37–47, Winter 2017.
- [32] R. Hult, M. Zanon, S. Gros *et al.*, "Optimisation-based coordination of connected, automated vehicles at intersections," *Veh. Syst. Dynamics*, vol. 58, no. 5, pp. 726–747, May 2020.
- [33] P. Tallapragada and J. Cortés, "Hierarchical-distributed optimized coordination of intersection traffic," *IEEE Trans. Intell. Transp. Syst.*, vol. 21, no. 5, pp. 2100–2113, May 2020.
- [34] A. I. M. Medina, F. Creemers, E. Lefeber *et al.*, "Optimal access management for cooperative intersection control," *IEEE Trans. Intell. Transp. Syst.*, vol. 21, no. 5, pp. 2114–2127, May 2020.
- [35] K. Dresner and P. Stone, "A multiagent approach to autonomous intersection management," *J. Artificial Intelligence Res.*, vol. 31, pp. 591–656, Mar. 2008.
- [36] M. Ahmane, A. Abbas-Turki, F. Perronnet *et al.*, "Modeling and controlling an isolated urban intersection based on cooperative vehicles," *Transp. Res. Part C: Emerging Technol.*, vol. 28, pp. 44–62, Mar. 2013.
- [37] W. Wu, J. Zhang, A. Luo *et al.*, "Distributed mutual exclusion algorithms for intersection traffic control," *IEEE Trans. Parallel Distrib. Syst.*, vol. 26, no. 1, pp. 65–74, Jan. 2015.
- [38] M. R. Hafner and D. Del Vecchio, "Computational tools for the safety control of a class of piecewise continuous systems with imperfect information on a partial order," *SIAM J. Control Optim.*, vol. 49, no. 6, pp. 2463–2493, Dec. 2011.
- [39] A. Colombo and D. Del Vecchio, "Least restrictive supervisors for intersection collision avoidance: A scheduling approach," *IEEE Trans. Autom. Control*, vol. 60, no. 6, pp. 1515–1527, Jun. 2015.

- [40] S. Glaser, B. Vanholme, S. Mammar *et al.*, “Maneuver-based trajectory planning for highly autonomous vehicles on real road with traffic and driver interaction,” *IEEE Trans. Intell. Transp. Syst.*, vol. 11, no. 3, pp. 589–606, Sep. 2010.
- [41] J. Lee and B. Park, “Development and evaluation of a cooperative vehicle intersection control algorithm under the connected vehicles environment,” *IEEE Trans. Intell. Transp. Syst.*, vol. 13, no. 1, pp. 81–90, Mar. 2012.
- [42] G. R. de Campos, P. Falcone, and J. Sjöberg, “Autonomous cooperative driving: A velocity-based negotiation approach for intersection crossing,” in *Proc. IEEE Int. Conf. Intell. Transp. Syst.*, vol. 1, The Hague, Netherlands, Oct. 2013, pp. 1456–1461.
- [43] M. A. S. Kamal, J. ichi Imura, T. Hayakawa *et al.*, “A vehicle-intersection coordination scheme for smooth flows of traffic without using traffic lights,” *IEEE Trans. Intell. Transp. Syst.*, vol. 16, no. 3, pp. 1136–1147, Jun. 2015.
- [44] N. Chohan, M. A. Nazari, H. Wymeersch *et al.*, “Robust trajectory planning of autonomous vehicles at intersections with communication impairments,” in *Proc. Ann. Allerton Conf. Commun., Control, and Comput.*, Monticello, USA, Sep. 2019, pp. 832–839.
- [45] F. Yang and Y. Shen, “Performance limit of two-agent scheduling with kinematic constraints,” in *Proc. IEEE Global Commun. Conf.*, Madrid, Spain, Dec. 2021, pp. 1–6.